2020

Paleoenvironments containing *Coryphodon* in the Fort Union and Willwood Formations Spanning the Paleocene-Eocene Thermal Maximum (PETM), Bighorn Basin, Wyoming

Emily N. Randall
The College of Wooster, erandall20@wooster.edu

Paleoenvironments containing *Coryphodon* in the Fort Union and Willwood Formations Spanning the Paleocene-Eocene Thermal Maximum (PETM), Bighorn Basin, Wyoming

by

Emily Randall

Submitted in partial fulfillment of the requirements

of Senior Independent Study at

The College of Wooster

February 20, 2020

Abstract

Preliminary data point toward a new hypothesis in which *Coryphodon* lived in wetter habitats before the Paleocene-Eocene Thermal Maximum (PETM), but was able to adapt to drier habitats in order to survive post-PETM. Early Paleogene nonmarine strata are extensively exposed in the Bighorn Basin of northwestern Wyoming. The Fort Union and Willwood Formations represent alluvial deposition within a Laramide Basin formed from the Paleocene through early Eocene. Therefore, the basin is an ideal place to study the local effects of the PETM, a rapid global warming event that occurred about 55.5 million years ago at the Paleocene–Eocene boundary. During this event, an initial decrease in rainfall was followed by wet and dry cycles with increased temperature and decreased precipitation. Some flora and fauna went extinct, but many others exhibited dwarfing during this interval. The response of the large mammal *Coryphodon* to the PETM is poorly understood, but is of special interest due to its inferred semiaquatic nature.

We collected 14 stratigraphic sections from 5 mammalian biozones within the Bighorn Basin, each centered around depositional units containing *Coryphodon*. The depositional environments of these units were evaluated by describing the grain size; matrix and mottling colors; mottling percent; abundance and type of nodules; shrink-swell features such as slickensides and clay cutans; and other interesting attributes such as organic matter, invertebrate fossils, sedimentary features, and mottling color or percentage stratigraphic changes. The depositional environments include ponds, swamps, fluvial deposits, soils with evidence of wet and dry cycles, and dry soils.

Acknowledgments

Funding for this study was provided by the Keck Geology Consortium and the National Science Foundation (NSF-REU1659322).

I would like to thank Dr. Mark Wilson for mentoring me through the process of researching, conducting, and writing my Independent Study. I would also like to thank him for his assistance in applying for this Keck Project.

Additionally, I would like to thank Dr. Michael D'Emic, Dr. Simone Hoffmann, and Dr. Brady Foreman for their mentorship throughout the project, and the Keck Wyoming team: Danika, Isaac, Richard, Michael, and Grant. I would also like to thank everyone at The Yellowstone Bighorn Research Association for their support during our fieldwork.

Finally, I would like to thank The College of Wooster Earth Sciences department for all of their support throughout this project.

Table of Contents

Introduction

The burning of fossil fuels supports many modern conveniences, but their emissions are also raising greenhouse gas concentrations in the atmosphere, which are increasing global temperature and therefore leading to global climate changes (Gingerich, 2019). The Paleocene-Eocene Thermal Maximum (PETM), a global warming event about 55.5 million years ago, can act as an analogy for future global warming if fossil fuel emissions continue their upward trend (Kraus and Riggins, 2007; Gingerich, 2019). The Bighorn Basin in Wyoming is one locality where PETM-aged rock units are exposed, which makes it an excellent location to study the environmental, floral, and faunal responses to this interval of increased temperature and decreased precipitation (Gingerich, 2003; Wing et al., 2005; Kraus and Riggins, 2007; Smith et al., 2008; Kraus et al., 2015).

As the Earth continues into a time of increasing temperature and changing climate, the PETM can offer insights into how modern-day flora and fauna might respond to these changes. Previous research has concluded that some key adaptations, such as dwarfing, helped certain fauna survive this rapid and large-scale global warming (Gingerich, 1989, 2003; Smith et al., 2008; Secord et al., 2012). However, it is unclear why some of these mammals, such as the genus *Coryphodon* which is hypothesized to be water-dependent, survived this much drier climate (Clementz et al., 2008; Secord et al., 2012).

Previous studies have argued that *Coryphodon* was semi-aquatic based on morphological features of their skeleton and enamel δ^{18}O values (Clementz et al., 2008). Therefore, my starting hypothesis is that *Coryphodon* will mainly be found in aquatic or semi-aquatic facies throughout the PETM interval.

Paleocene-Eocene Thermal Maximum (PETM)

The Paleocene-Eocene Thermal Maximum (PETM) was a roughly 150,000-year interval about 55.5 million years ago during which there was a massive release of carbon into the atmosphere. This led to a rapid global warming of 5-8°C over less than 20,000 years, with persistently high temperatures for the remainder of the event (Wing et al., 2005; Kraus and Riggins, 2007; McInerney and Wing, 2011; Gingerich, 2019). Therefore, it can serve as an analog for the possible impacts of modern climate change, since the PETM is thought to be mostly due to CO_2-driven rather than orbital forcing mechanisms of Late Cenozoic glacial-interglacial climate changes (Abels et al., 2016; Gehler et al., 2016). It has been found that modern rates of carbon emissions are 9-10 times higher than those during the onset of the PETM, and, if this upward trend of anthropogenic emissions continues, PETM-scale carbon accumulation in the atmosphere could be reached in as few as 140-259 years, or about 5-10 human generations (Gingerich, 2019). Therefore, it is imperative to learn as much as we can about analogous times in the past, such as the PETM, in order to better understand the impacts that anthropogenically driven climate change could have on our modern world.

While a substantial amount is understood about the effects of the PETM globally, in large part due to modeling (i.e. Carmichael et al., 2017; Kiehl et al., 2018), much less is known about it regionally. Recently, researchers have begun examining PETM-aged sites on a fine stratigraphic scale to better determine its regional effects. Some of these effects include altered climates, ecosystems, and ocean chemistry as well as floral changes and species dwarfing (Wing et al., 2005; Kraus and Riggins, 2007; D'Ambrosia et al., 2017; Schmidt et al., 2018). One area where these regional effects have been studied for decades in great detail, the Bighorn Basin of Wyoming, is the research area of this study.

Study Area

The northern Bighorn Basin, specifically its well-exposed Fort Union and Willwood Formations in the Sand Coulee area, are the focus of this study. This basin is intermontane, meaning surrounded by mountains, and was formed during the Laramide Orogeny (~65-35 Ma) within the foreland basin of the earlier Sevier Orogeny (Mackin, 1937; Dickinson et al., 1988; DeCelles, 2004) (Figure 1). The Pryor Mountains are located to the northeast, the Bighorn Mountains to the east, the Owl Creek and Bridger Mountains to the south, and the Absaroka and Beartooth Mountains to the west (Mackin, 1937). These surrounding mountain ranges have provided most of the sediment in the basin, though the vast majority of orogenic activity had ceased before the deposition of the Lower Eocene Willwood Formation. Additionally, at the time being studied, the basin was open to the north with water flowing in that direction (Kraus and Riggins, 2007; Kraus et al., 2015).

The Sand Coulee area of the basin, where our specimens are from, has been previously subdivided into a multitude of fossil localities by Gingerich (2001). Specimens collected during our fieldwork were assigned to these localities based on GPS coordinates and elevation data (Figure 2) (Table 1).

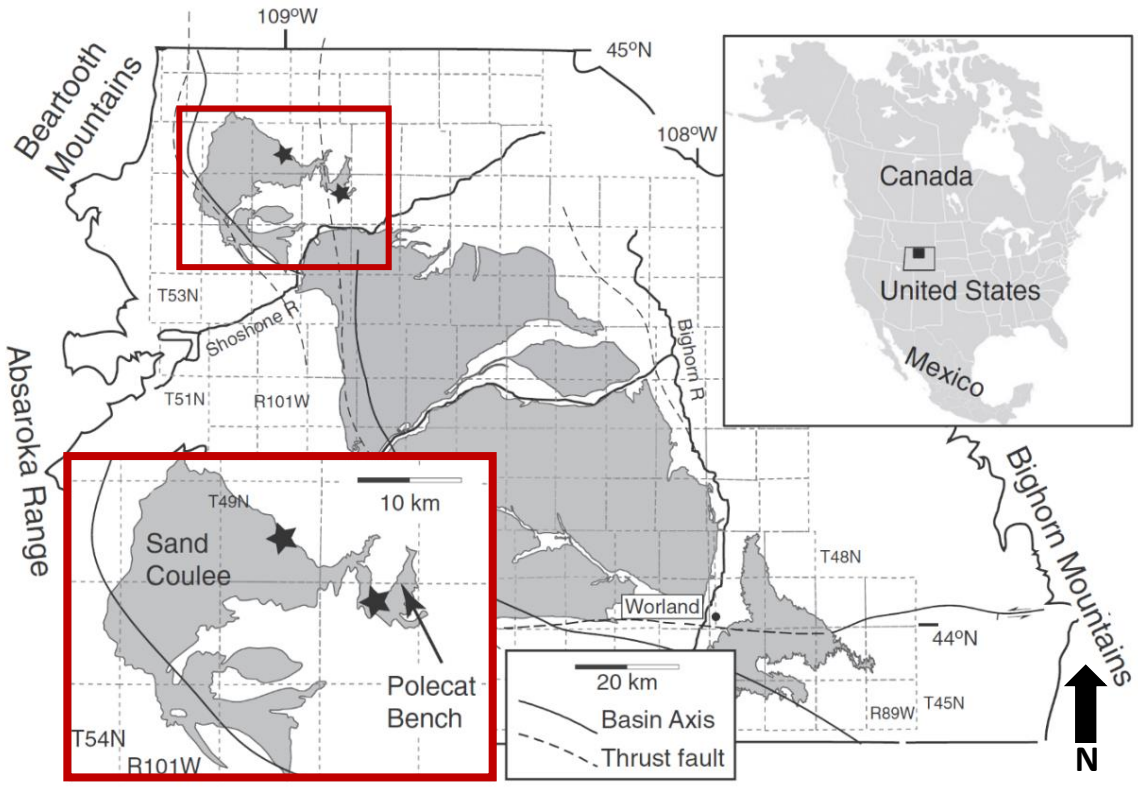

Figure 1. Map of the Bighorn Basin with the exposed Willwood Formation highlighted in gray. Inset shows the study area in the northern part of the basin with stars highlighting important sites. Polecat Bench is where most of the previous studies examining the PETM stratigraphy have occurred and Sand Coulee is where this study's samples are from (Modified from Kraus et al., 2015, Figure 1).

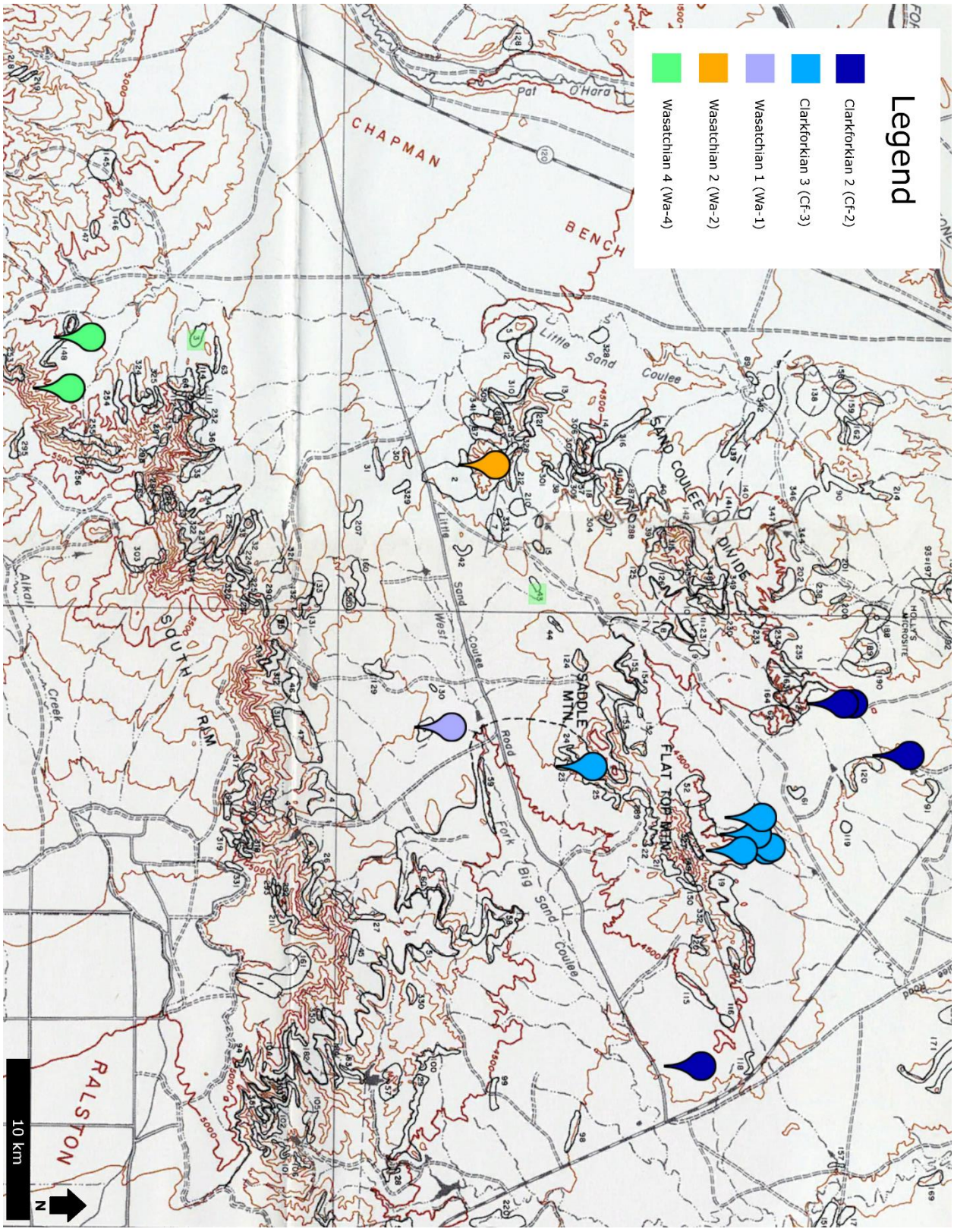

Figure 2. Map showing our specimens in relation to the Gingerich (2001) localities (Modified from Gingerich and Klitz, 1985).

Sampling Location	Formation (Epoch)	*Coryphodon* Fossils	Biozone	Gingerich Locality	Meters Above K-Pg Boundary
CORY 19-13	Willwood (Paleocene)	Parts of femur and phalanges	Cf-3	Between 52, 53, and 334	1405
CORY 19-22	Willwood (Paleocene)	Complete tibia	Cf-3	53	1405
CORY 19-23	Willwood (Paleocene)	*Coryphodon*? - canine, phalanx, and other bones	Cf-3	53	1405
CORY 19-29	Willwood (Paleocene)	Skull with ulna	Cf-3	53	1405
CORY 19-32	Willwood (Paleocene)	Canine, pelvis, vertebrae & other small mammals, crocodile, turtle	Cf-3	53	1405
CORY 19-34	Willwood (Paleocene)	Post crania	Cf-2	Between 61 and 127	1335-1355
CORY 19-35	Willwood (Paleocene)	Teeth & skull fragments	Cf-2	Between 98, 115, 116, and 118	1300-1370
CORY 19-52	Willwood (Paleocene)	Teeth	Cf-2	127	1355

Sampling Location	Formation (Epoch)	*Coryphodon* Fossils	Biozone	Gingerich Locality	Meters Above K-Pg Boundary
CORY 19-53	Willwood (Paleocene)	Teeth	Cf-2	120	1300
CORY 19-54	Willwood (Eocene)	Post crania, humeral head, proximal tibia, tarsal, distal ulna & other small mammal bones	Cf-3	23	1495
CORY 19-57	Willwood (Eocene)	Skeleton	Wa-4	Between 148, 253, 294, and 295	1505-2250
CORY 19-58	Willwood (Eocene)	Exploded skeleton	Wa-1	Near 6 and 130	1530-1540
CORY 19-59	Willwood (Eocene)	Teeth	Wa-4	Between 148 and 253	2050-2095
CORY 19-67	Willwood	Femur, humerus, and tooth fragments	Wa-2	2	1720

Table 1. Information on the location of each stratigraphic section and the fossils it contained. Gingerich localities and measurements above the K-Pg boundary are from Gingerich, 2001. Detailed field notes on these stratigraphic sections can be found in the appendix. Locality information for these sites is on file at the University of Michigan Museum of Paleontology and available upon request.

Stratigraphy

The Paleocene-Eocene boundary in the Bighorn Basin is characterized by two formations: the Paleocene Fort Union Formation and the Lower Eocene Willwood Formation. In the northern part of the Bighorn Basin, where this study occurred, the combination of these formations is about 2,000 meters thick (Kraus and Wells, 1999; Kraus et al., 2015). They were deposited in the basin during the Laramide Orogeny, which occurred due to subduction on the west coast of North America from about 65 to 35 Ma. This orogeny was caused by the weakened subduction of the Farallon Plate, which led to a flattened out, lower angle of subduction. This pushed melting and volcanism further eastward than it was during the Sevier Orogeny and caused the initial uplift of the Rocky Mountains and Colorado Plateau (Copeland et al., 2017; Blakey and Ranney, 2018). This change in subduction angle also caused a shift from the horizontally-directed thin-skinned deformation characteristic of the Sevier Orogeny to a thick-skinned deformation that involved basement-cored vertical uplifts of the Precambrian basement rock (Dickinson et al., 1988; Blakey and Ranney, 2018). The compressive stress from the subducting plate caused a reactivation of older Precambrian and Phanerozoic faults as well as created new faults in zones of weakness. This tectonic activity uplifted the floor of the Bighorn Basin some as well as the mountain ranges that surround it, with the exception of the Absarokas (Mackin, 1937; Seeland, 1998).

Both formations are mudrock-dominated with three major facies: thick, laterally extensive sheet sandstones; heterolithic (interbedded sand and mud) deposits with ribbon sandstones surrounded by mudrocks with weakly developed paleosols; and fine-grained deposits with moderately to strongly developed paleosols (Figure 3) (Kraus and Riggins, 2007). These paleosols, which are common in both formations but vary greatly in color, can provide

significant information about the depositional history and paleoenvironments of the interval spanning the PETM.

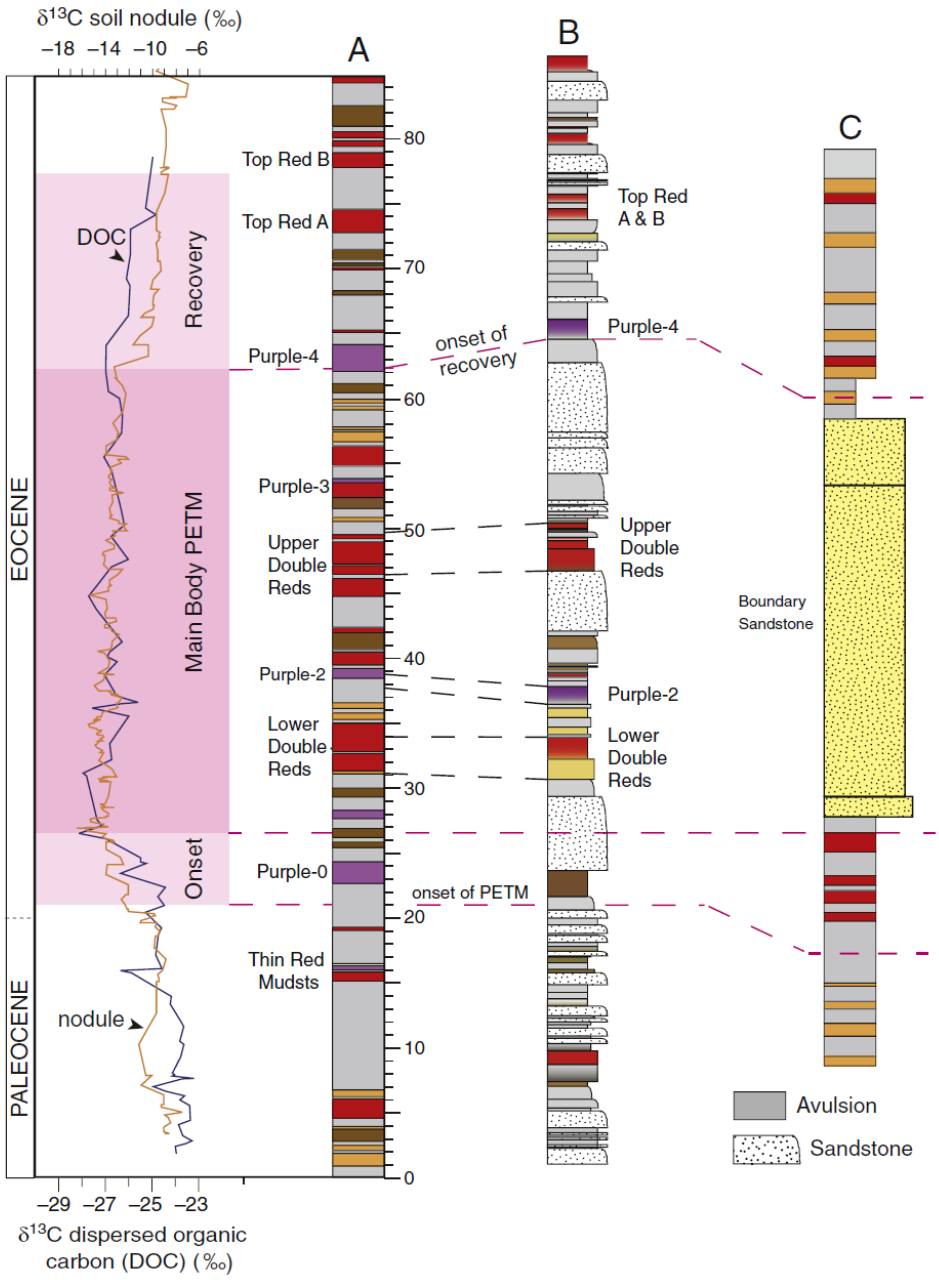

Figure 3. Stratigraphic columns showing the (A) Polecat Bench paleosols, (B) Polecat Bench core section obtained during the Bighorn Basin Coring Project, and (C) Sand Coulee area, which is the location of the Boundary Sandstone. The sedimentary layers consist of colorful paleosols, avulsion deposits, and sandstones. The pedogenic carbonate $\delta^{13}C$ curve (orange) was used to subdivide the PETM onset, main body, and recovery in relation to the stratigraphy (Kraus et al., 2015, Figure 2).

Fort Union Formation

The Paleocene Fort Union Formation directly underlies the Willwood Formation and, while in some areas it is located tens of meters below the stratigraphic occurrence of the PETM interval, in others their boundary almost exactly intersects the PETM. The Fort Union has mainly been dated biostratigraphically (Gingerich, 1976, 1980; Rose, 1980), though Butler et al. (1981) used magnetostratigraphy to correlate the Polecat Bench area of the formation with the Cenozoic magnetic polarity time scale.

The formation is about 1,050m thick in the northern section of the basin where it is fully exposed due to Pleistocene-Holocene erosion. Its paleosols are well-developed, but predominately gray in color, as they are depleted in iron relative to the red and purple paleosols of the Willwood Formation (Kraus and Wells, 1999; Kraus and Riggins, 2007). Overall, the thickness of this formation, which is greater than 7,500 ft in the center of the basin, indicates that there was continued subsidence of the basin during the Laramide Orogeny (Clyde et al., 2007; Finn, 2010). Its grey paleosols give the Fort Union Formation a drab appearance next to the overlying Willwood Formation, which makes them relatively easy to distinguish in the field (Butler et al., 1981).

Willwood Formation

The Lower Eocene Willwood Formation has been dated to approximately 55 to 52 Ma. This dating was accomplished by correlating a combination of biostratigraphic and magnetostratigraphic data with the geomagnetic timescale (Tauxe et al., 1994; Secord et al., 2006; Clyde et al., 2007).

The formation consists of a thick (~780 m) alluvial floodplain successional deposit. The formation itself is characterized by red, candy cane-like, banding (Bown and Gingerich, 1980; Butler et al., 1981). Overbank and avulsion deposits dominate the formation, with channel-belt sandstones making up less than 10% of the stratigraphy (Kraus et al., 2015). However, the Boundary Sandstone, an unusually thick and laterally continuous fluvial sand body that was likely deposited due to short-term climate alterations, is an exception with a maximum thickness of 33 meters and a mean thickness of 16.3 meters (Foreman, 2014). The floodplain paleosols of the Willwood Formation can be distinguished by their well-developed red; yellow-brown; and purple colors, which are not found in the northern part of the basin where our fieldwork was conducted (Kraus and Riggins, 2007; Kraus et al., 2015).

PETM Environments

The paleoenvironment of the northern Bighorn Basin changed continually throughout the PETM and post-PETM recovery interval. An initial decrease in rainfall of about 40% occurred at the beginning of the PETM. This was followed by a cycle of wet and dry intervals that suggest increased temperature and water stress to local flora and fauna. Eventually, a recovery interval was reached with a reappearance of a more humid climate, characterized by a return to pre-PETM precipitation levels and cooler temperatures (Wing et al., 2005; Kraus and Riggins, 2007; Foreman, 2014; Kraus et al., 2015).

Paleosols

Differences in paleosol color, and the sedimentary features found within them, are key to interpreting the precipitation of intervals pre, during, and post PETM in the northern Bighorn

Basin. Paleosols differ in color due to oxygen availability and iron content when they were produced. Paleosol color in the basin, in decreasing order of precipitation, is gray, purple (rare in the northern part of the basin), brown (rare), yellow-brown, and red (Kraus and Riggins, 2007). Therefore, the stratigraphic occurrence of these paleosol colors can be used to interpret precipitation throughout the Paleocene Fort Union and Lower Eocene Willwood Formations (Figure 4).

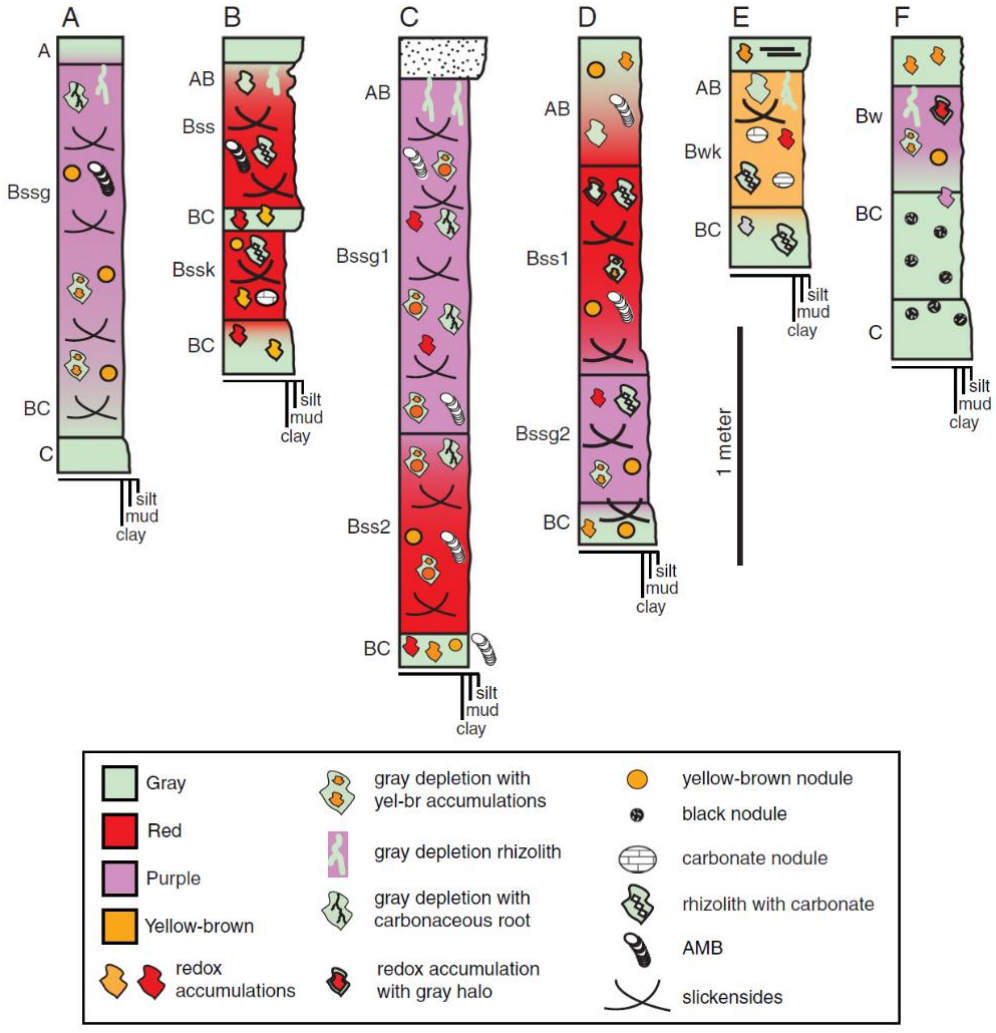

Figure 4. Stratigraphic sections showing the major types of paleosols present in the Bighorn Basin around the PETM. Other sedimentary features are also represented within the paleosols. A, B, C, D, and E illustrate sections of the Willwood Formation and F exemplifies a section of the Fort Union Formation (Kraus et al., 2013, Figure 3).

Other Sedimentary Features

Additional sedimentary features within the paleosols can also be used to interpret precipitation around and during the PETM. These include nodules; mottles; and slickensides, which indicate times of wetting and drying (Kraus and Riggins, 2007). Root traces and rhizohaloes, root traces that would not be visible without a change in soil color, are also present (Figure 5) (Kraus et al., 2015).

Two types of nodules are present in the paleosols of the Fort Union and Willwood Formations: yellow-brown siderite and carbonate. The presence of yellow-brown siderite nodules in soils indicates wetter conditions. Schwertmann and Fanning (1976) identified that an increase in the abundance and size of these nodules occurs as soil moisture increases, but they are absent from very poorly drained soils. Carbonate nodules form in drier conditions, though their development is slightly more complex (Adams et al., 2011). However, they are more common in soils from areas with seasonal climates that have an estimated mean annual precipitation of < 760mm (Royer, 1999) to < 1000mm (Retallack, 1994).

Matrix chroma, a measure of the saturation of a color in the Munsell Color Chart, has also been shown to decrease as the length of time a soil is saturated increases. Matrix colors with a particularly low chroma (≤ 2) are commonly associated with seasonal saturation and gleying, the process of waterlogging and oxygen reduction, of soils (Evans and Franzmeier, 1986; Veneman et al., 1998; Adams et al., 2011). It should be noted that there has been some debate about the amount that paleosol colors reflect pedogenesis, the process of soil formation, versus burial diagenesis, chemical and physical changes to the sediment post-deposition during its conversion to a sedimentary rock (Retallack, 1991; Blodgett et al., 1993; PiPujol and Buurman, 1994; Adams et al., 2011). However, chroma has still been shown to be useful in determining

poorly drained versus well-drained and oxygenated conditions in some paleosol studies, such as some relatively recent ones in the Bighorn Basin (e.g., Adams et al., 2011; Kraus et al., 2013)

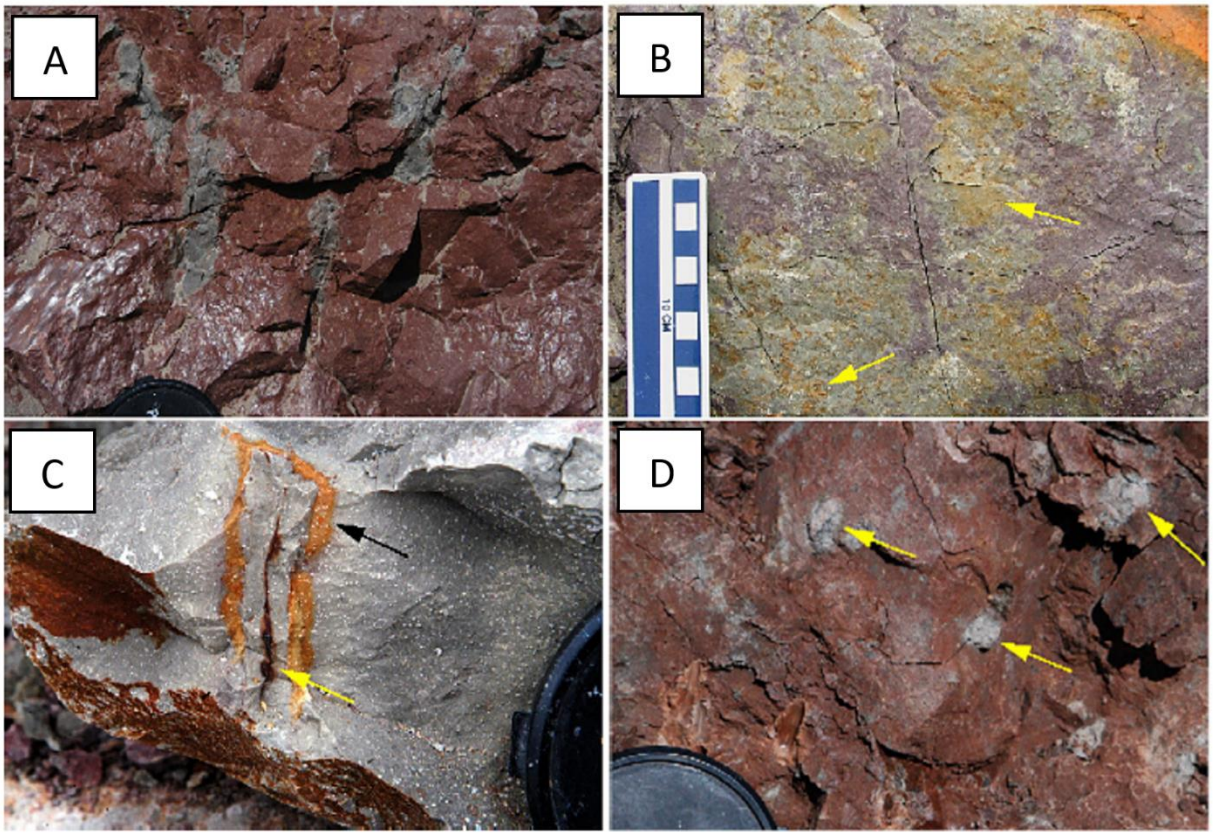

Figure 5. (A) Elongated gray mottles, likely rhizohaloes, in a red paleosol. Lens cap (64 mm diameter) for scale. (B) Yellow-brown nodules and mottles, shown with yellow arrows, embedded in gray mottles. All within a purple paleosol. (C) Gray rhizolith with a carbonaceous core (yellow arrow) surrounded by a yellow-brown rim (black arrow) in a gray paleosol. Lens cap for scale. (D) Carbonate nodules, shown with yellow arrows, in a red paleosol. Lens cap for scale (Modified from Kraus and Riggins, 2007, Figure 3).

Paleontology

Changing environments during the PETM resulted in changes in species diversity and habits within the Bighorn Basin. Examining paleosols and other sedimentary features can allow for a more precise interpretation of how the local environment changed throughout the PETM.

Transient changes in vegetation composition during the PETM show a shift from temperate paleofloras to flora characteristic of dry tropical and subtropical areas. This has been deduced by examining floral leaf margins and areas, to determine mean annual temperature and mean annual precipitation respectively (Wing et al., 2005). The flora taxa was also a mixture of native species and those that migrated to the area during the environmental changes of the PETM (Wing et al., 2005; D'Ambrosia et al., 2017).

Invertebrates were also present in the basin during the PETM. Freshwater crayfish burrows, of the ichnospecies *Camborygma litonomos*, have been found in the Willwood Formation paleosols at Polecat Bench. Modern crayfish that construct similar burrows often do so to escape desiccation in areas with fluctuating water tables. Therefore, a sharp decrease in these burrows throughout the PETM suggests significantly improved soil-drainage and lower water tables on the Willwood floodplain (Figure 6) (Smith et al., 2008).

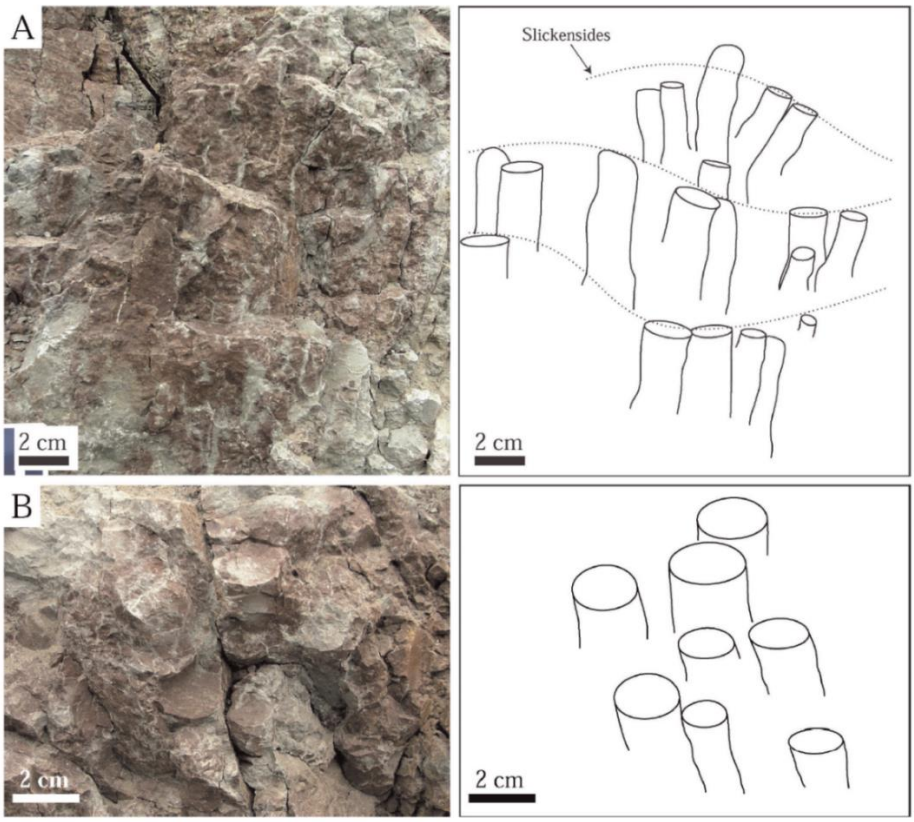

Figure 6. Outcrop views of prismatic soil structures, interpreted as freshwater crayfish burrows, with line drawings of the structures. Solid lines trace the individual prisms and dotted lines show slickensides (Smith et al., 2008, Figure 4).

Previous research has shown that the size and behavior of soil invertebrates changed drastically during the PETM (Smith et al., 2009). Increased burrows from insects and oligochaetes (earthworms) have been found, as well as a decrease in crayfish burrows and molluscan body fossils. The former suggests longer soil development and increased drainage conditions while the latter is likely due to drier floodplain conditions and lower water tables. Overall, burrow diameters of a wide variety of soil invertebrates decreased by 30-46% during the PETM interval. With burrow size acting as an analogy for body size, this represents a major dwarfing of invertebrate soil fauna during this time (Smith et al., 2009).

Mammals

Many modern mammalian orders of North America first appeared close to the Paleocene-Eocene transition, these include Rodentia (rodents), Chiroptera (bats), Primates, Artiodactyla (even-toed ungulates, hooved animals, such as cattle and deer), and Perissodactyla (odd-toed ungulates, such as horses and rhinos) (Gingerich, 1989).

The Bighorn Basin and adjoining Clarks Fork Basin in northwestern Wyoming contain one of the most complete and best-studied stratigraphic sections of continental Paleocene and early Eocene sediment in the world. The Clarkforkian-Wasatchian boundary is of particular interest in this area, as it closely coincides with the Paleocene-Eocene boundary. North American Paleogene land-mammal ages consist of three and seven mammalian biozones respectively, and are preceded by the six mammalian biozones of the Tiffanian. The beginning of the Clarkforkian can be distinguished in the rock record by the first appearance of Rodentia. Additionally, fossils of the pantodont *Coryphodon* are common during this land-mammal age. The Clarkforkian land-mammal age ends with the first appearance of perissodactyl fossils. The beginning of the Wasatchian land-mammal age is also characterized by the first appearance of Artiodactyla and Primates (Gingerich, 1989, 2003).

Dwarfing appears to have been a common evolutionary response of some mammals to past global warming events, such as the PETM. The extent of the dwarfing also seems to have been related to the magnitude of the event (Secord et al., 2012). Rising temperatures and drought, as well as decreasing nutrient availability, may have had a direct impact on the body size of large mammals in the Bighorn Basin during the PETM, possibly by decreasing primary productivity in their plant food sources or simply decreasing their biomass production. This could be supported by the occurrence of a dwarfing recovery of about 76% in early horses during

the PETM recovery interval (Wing et al., 2005; Kraus and Riggins, 2007; Secord et al., 2012; D'Ambrosia et al., 2017).

The genus of interest in this study is *Coryphodon* (Suborder Pantodonta, Superfamily Coryphodontoidea, Family Coryphodontidae), which was a large herbivorous mammal (Figure 7) (Simons, 1960; Secord et al., 2012). *Coryphodon* was also the first mammalian megaherbivore (body mass > 1000 kg), reaching sizes up to that of a small rhinoceros (Uhen and Gingerich, 1995). Additionally, previous analysis of their enamel δ^{18}O values found that *Coryphodon* was probably water-dependent or even semi-aquatic and therefore aridity-insensitive (Clementz et al., 2008; Secord et al., 2012).

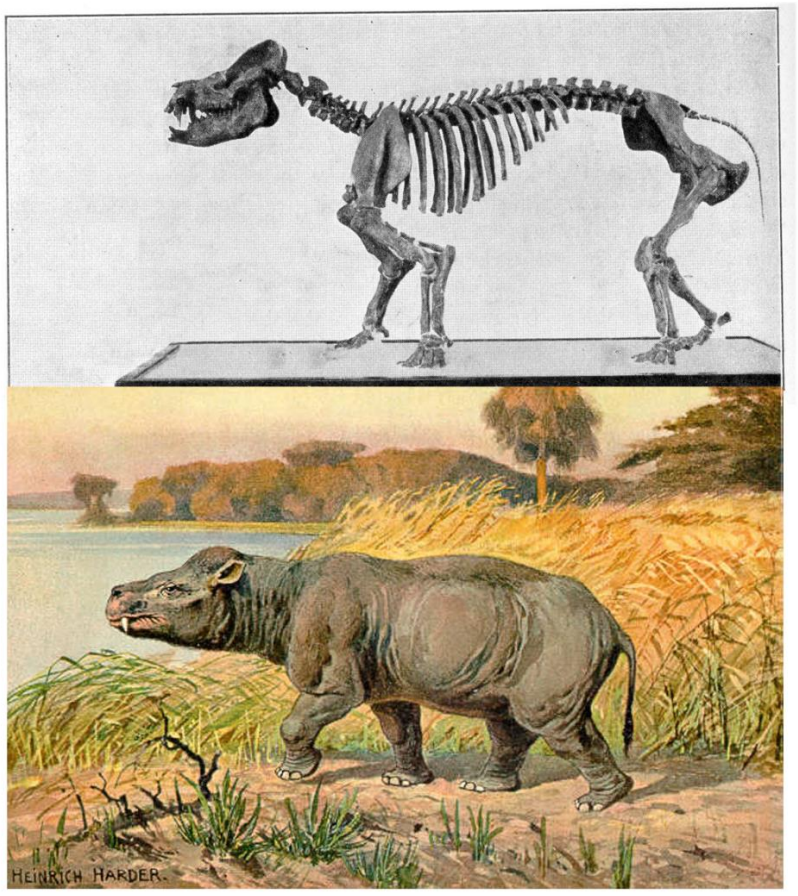

Figure 7. *Coryphodon* skeleton and an artistic interpretation of the genus by Heinrich Harder. (Images from http://www.copyrightexpired.com/earlyimage/bones/sharp/display_osborn_coryphodon.htm and http://www.copyrightexpired.com/Heinrich_Harder/coryphodon.html).

Summary of Background Information

The PETM was a time of intense, rapid global warming about 55.5 million years ago, which can be used as an analogy for the modern climate that will be reached in 5-10 human generations if the current upward trend of fossil fuel emissions continues (Wing et al., 2005; Kraus and Riggins, 2007; Gingerich, 2019). Wyoming's Bighorn Basin is an ideal location to study the PETM's local effects on sedimentation, precipitation, flora, and fauna. In this area, there was an initial decrease in rainfall followed by wet and dry cycles with increased temperature and water stress to local species. Finally, a recovery interval was reached where precipitation returned to pre-PETM levels and temperatures cooled. These events are reflected by changes in local paleosols, sedimentary features, flora, and fauna (Gingerich, 2003; Wing et al., 2005; Kraus and Riggins, 2007; Smith et al., 2008; Kraus et al., 2015).

While some fauna went extinct in response to the changing climate, others responded by dwarfing. *Coryphodon,* a large herbivorous mammal and the first mammalian megaherbivore, is a species that responded by dwarfing and is relatively common in the basin (Simons, 1960; Uhen and Gingerich, 1995; Secord et al., 2012). Therefore, it is the focus of this study. Previous studies have suggested that *Coryphodon* was semi-aquatic based on morphological features of their skeleton and enamel $\delta^{18}O$ values (Clementz et al., 2008). Therefore, I hypothesize that *Coryphodon* will mainly be found in aquatic or semi-aquatic facies throughout the PETM interval.

Methods

Field Methods

Data for this study were collected in the Sand Coulee area of the northern Bighorn Basin, more specifically in the Gingerich (2001) localities from Table 1. Care was taken to prospect for samples in a range of biozones surrounding the PETM in order to gain a broader insight into *Coryphodon* during this interval. The data consist of 14 stratigraphic sections in total, each of which contains a *Coryphodon* bearing unit. Of these, 11 contained fossil in situ and 3 were hypothesized to be the bone-bearing layer due to where the highest in-situ fossil was found and a comparison of bone color and preservation with unit matrix and mottling colors as well as grain size. Sections were measured by digging down to unweathered bedrock in ~0.5-meter-wide trenches (Figures 8 & 9). The following features were observed for each unit: thickness; grain size; matrix and mottling colors (using a Munsell Color Chart); mottling percent; abundance and type of nodules; shrink-swell features such as slickensides and clay cutans; lower contacts; and interesting attributes such as organic matter, invertebrate fossils, sedimentary features, and mottling color or percentage changes throughout the unit (Figure 10 & 11).

Figure 8. Trenched and cleaned stratigraphic section CORY 19-59 in the field before analysis.

Figure 9. Measuring units in stratigraphic section CORY 19-35 using a Jacob's staff.

Figure 10. Observing hand samples from stratigraphic section CORY 19-58 to determine grain size, matrix color, mottling color, and mottling percent.

Figure 11. A large amount of variability was observed between different stratigraphic units, specifically with respect to mottling color and percent. For example, the left image shows a rock with a fair amount of yellowish and purplish-red mottling from stratigraphic section CORY 19-54, while the right image is of a rock with very little orangish-brown mottling from stratigraphic section CORY 19-13.

Soil Morphology Index (SMI) Calculation

Using the methods described in Adams et al. (2011) and the Excel file provided in Appendix 1 of Kraus et al. (2013), a soil morphology index (SMI) number was calculated for each paleosol unit, which describes the soil moisture at the time of deposition for each unit. The factors which are important for calculating this number are matrix chroma (using the Munsell Color Chart), carbonate nodules, and yellow-brown siderite nodules. This index can be used to determine changes in drainage throughout the stratigraphic section as well as changes in drainage between the units where *Coryphodon* was found.

A scoring system, created by Adams et al. (2011), was used to calculate the SMI number of each claystone, mudstone, and siltstone unit. Matrix chroma ranged from 1 to 3 in the sampled units, therefore the minimum points assigned for this category was 1 and the maximum 3. The presence, size, and abundance of carbonate nodules and yellow-brown siderite nodules were then scored using Adams et al. (2011) Table 2 (Table 2), receiving either 0, 3, or 6 points for each of the two types of nodules. These three numbers were then summed for each unit to determine the SMI number of that unit.

	Wetter soil conditions	Intermediate conditions	Drier soil conditions
Features	0 points	3 points	6 points
Soil carbonate	no carbonate	Calcareous rhizoliths small (<mm) nodules	Larger (>mm) nodules
Yellow-brown nodules	Common to abundant	Sparse	Absent

Table 2. Points assigned in the soil morphology index (SMI) calculation based on the presence, size, and abundance of carbonate nodules and yellow-brown siderite nodules in the sampled units (Adams et al., 2011, Table 2).

Stratigraphic Column Creation

Stratigraphic columns were created in Adobe Illustrator. U.S. Geological Survey lithology patterns (Illustrator swatches) were used to differentiate rock types. Matrix and mottling colors were derived from the Munsell Color Chart. The percentage of mottling was roughly portrayed by the number of mottling shapes present in the unit.

RGB values were determined for the Munsell Color Chart using the Virtual Online Color Wheel created by Andrew Werth, which is a visual representation of RGB values calculated by The Munsell Color Science Laboratory (http://www.andrewwerth.com/color/). Since exact RGB equivalents only exist for Munsell colors with even chroma, the other representative colors were estimated. To do this, Munsell colors with exact RGB equivalents were blended in Illustrator using the blending tool to generate RGB representative colors for the Munsell colors with no exact RGB equivalent (i.e. a neutral chroma and a chroma of 2 to create a color for a chroma of 1 or a chroma of 2 and a chroma of 4 to create a color for a chroma of 3).

Results

Stratigraphic Columns

Stratigraphic columns were created for each section and grouped by mammalian biozone. Clarkforkian 2 is represented by columns 19-34, 19-35, 19-52, and 19-53 (Figures 13-16); Clarkforkian 3 is represented by columns 19-13, 19-22, 19-23, 19-29, 19-32, and 19-54 (Figures 17-22); Wasatchian 1 is represented by column 19-58 (Figure 23); Wasatchian 2 is represented by column 19-67 (Figure 24); and Wasatchian 4 is represented by columns 19-57 and 19-59 (Figures 25 and 26). An overall legend was also created to be used with all stratigraphic columns (Figure 12). Detailed field notes on these stratigraphic sections can be found in the appendix.

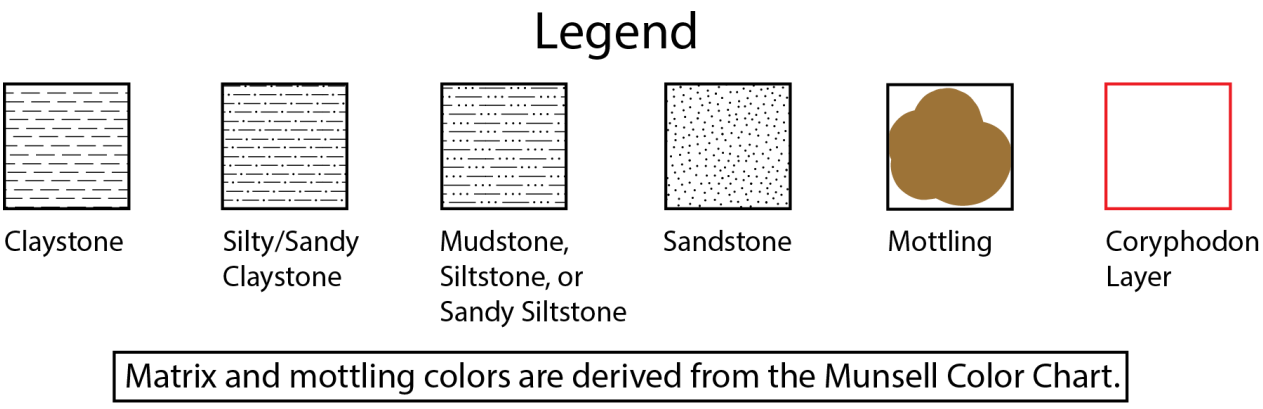

Figure 12. Legend for the following stratigraphic columns.

Clarkforkian 2

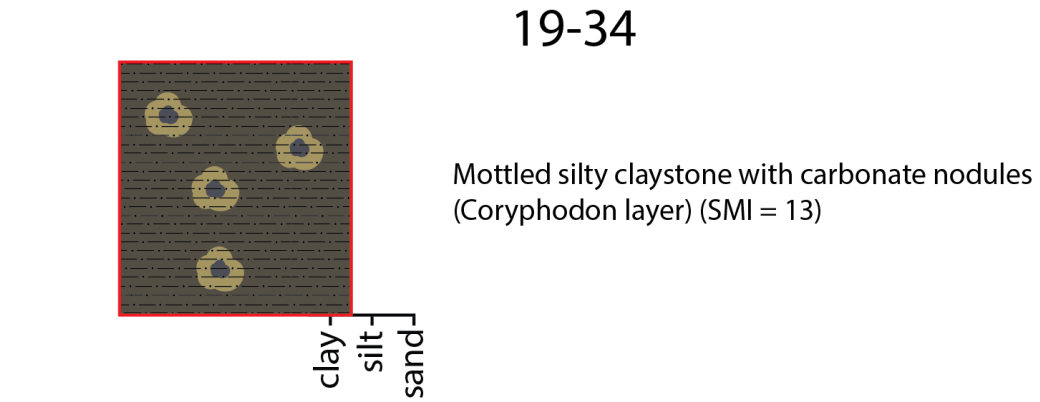

Figure 13. Column is CORY 19-34. The thickness of this unit is unknown. See figure 12 for legend.

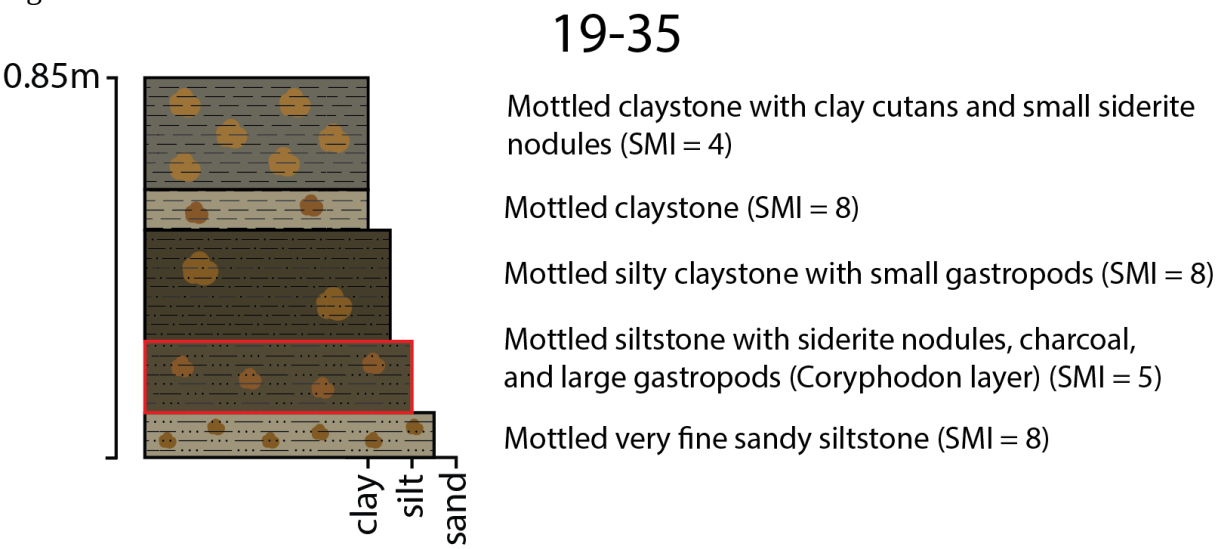

Figure 14. Column is CORY 19-35. See figure 12 for legend.

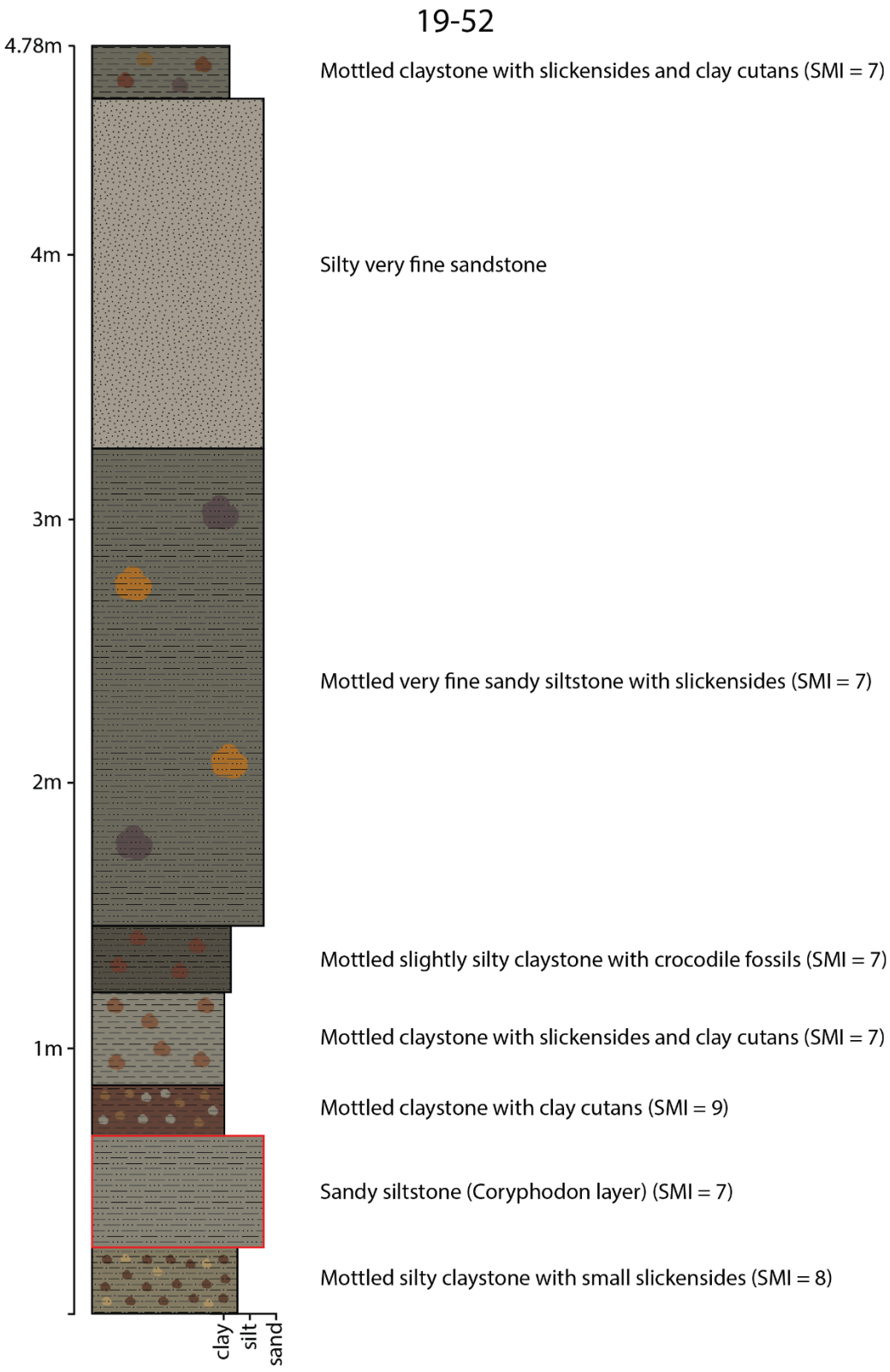

Figure 15. Column is CORY 19-52. See figure 12 for legend.

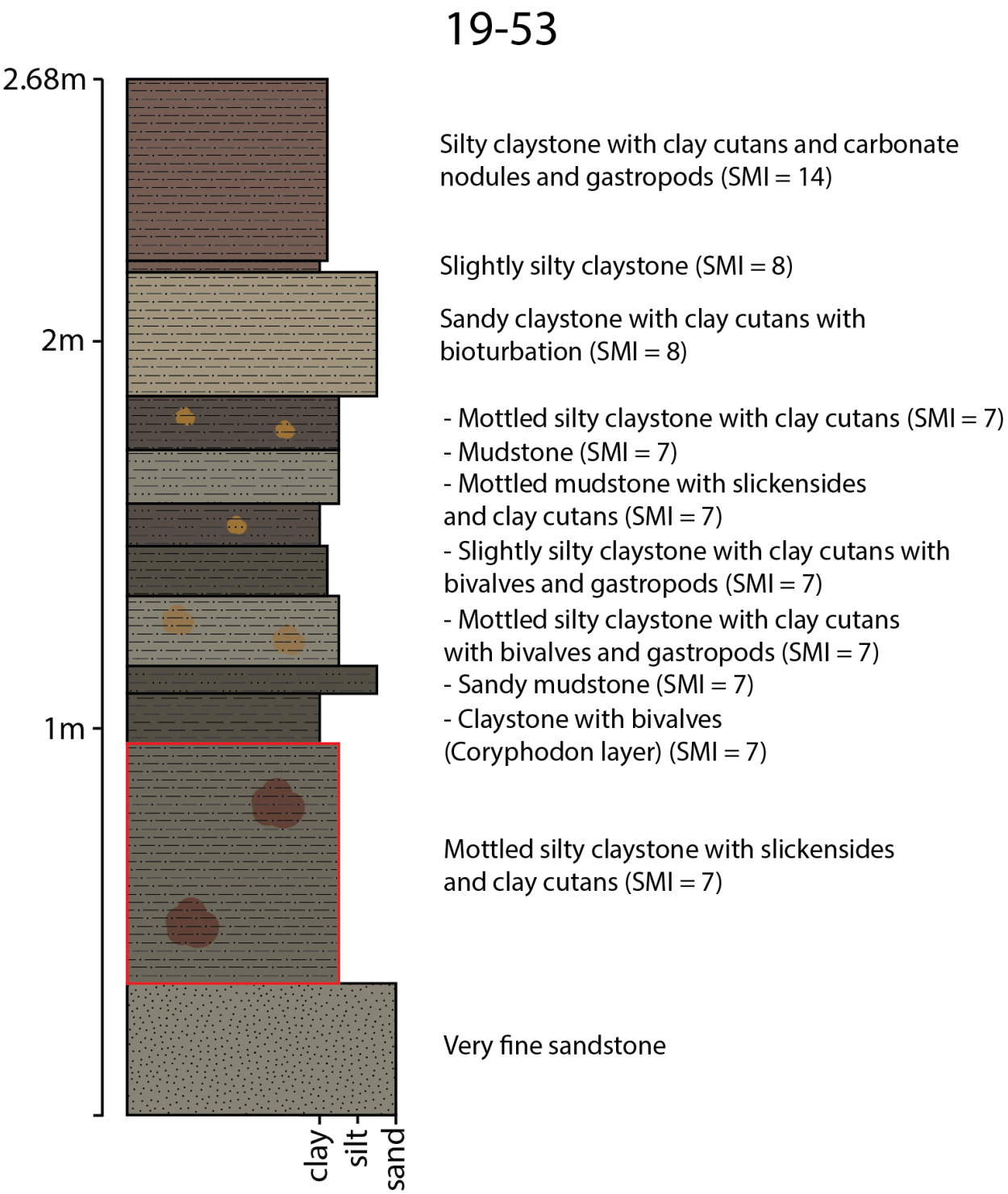

Figure 16. Column is CORY 19-53. See figure 12 for legend.

Clarkforkian 3

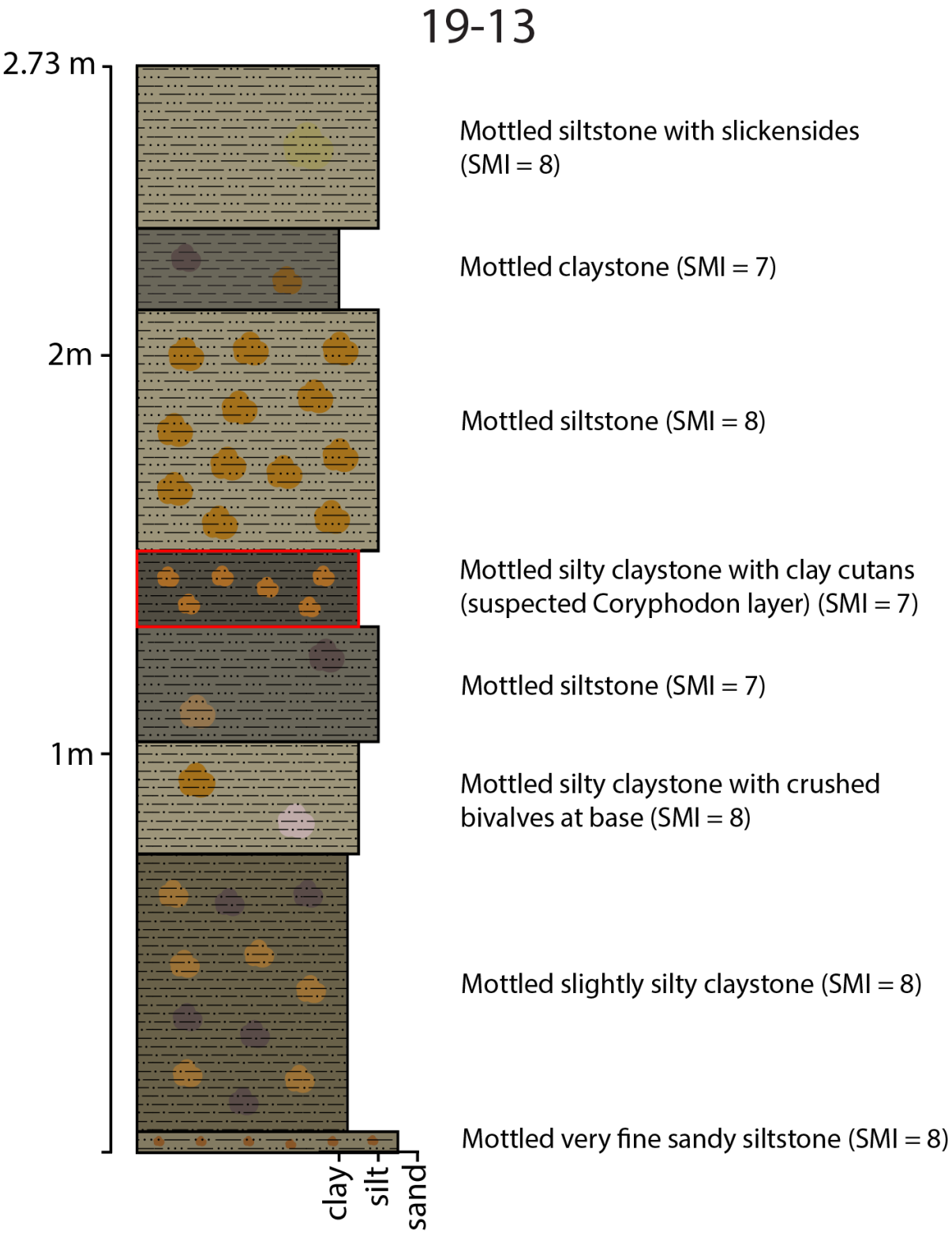

Figure 17. Column is CORY 19-13. See figure 12 for legend.

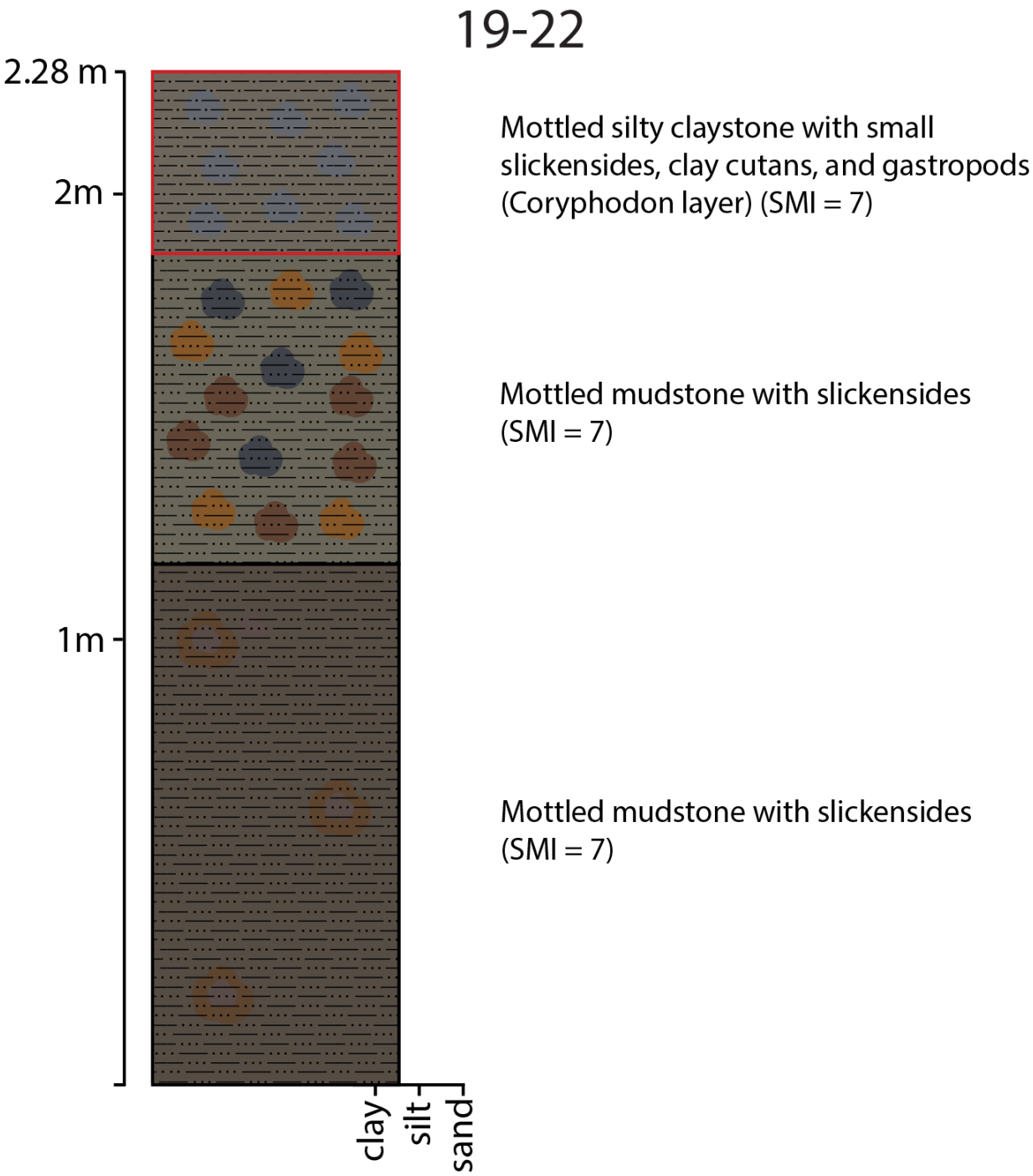

Figure 18. Column is CORY 19-22. See figure 12 for legend.

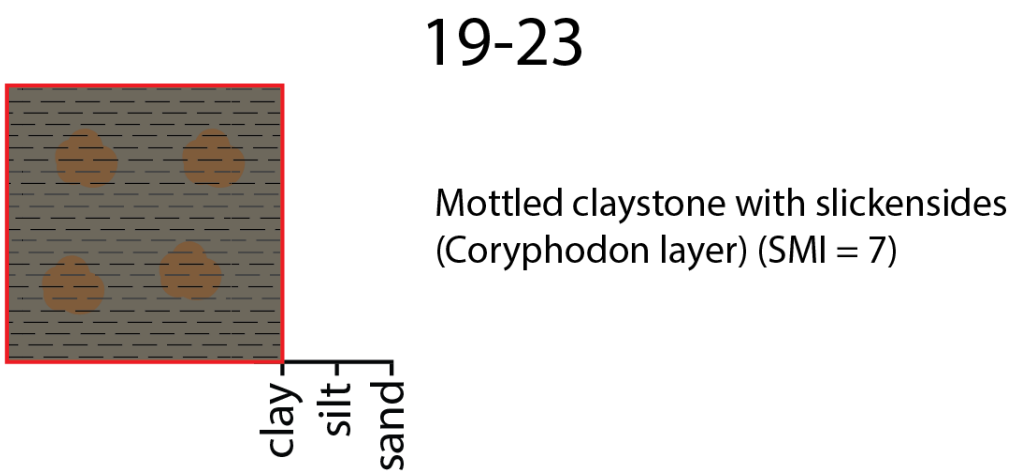

Figure 19. Column is CORY 19-23. The thickness of this unit is unknown. See figure 12 for legend.

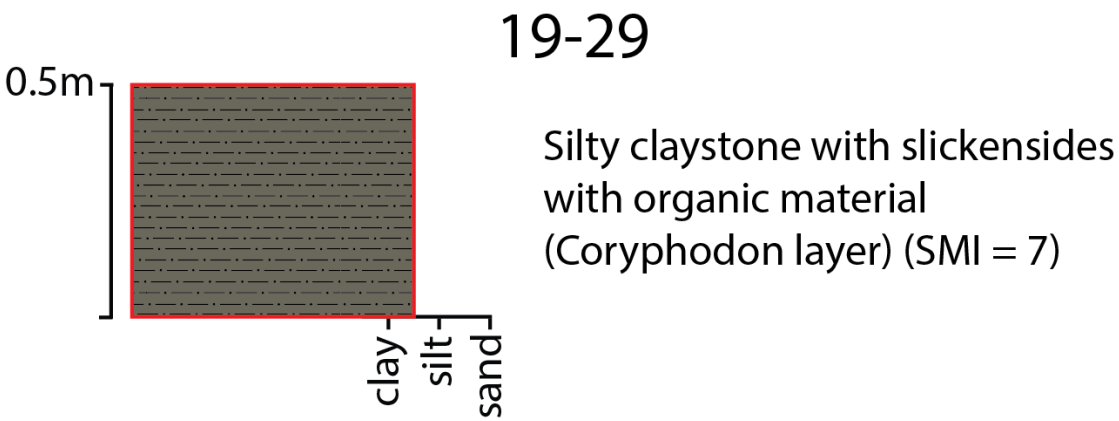

Figure 20. Column is CORY 19-29. See figure 12 for legend.

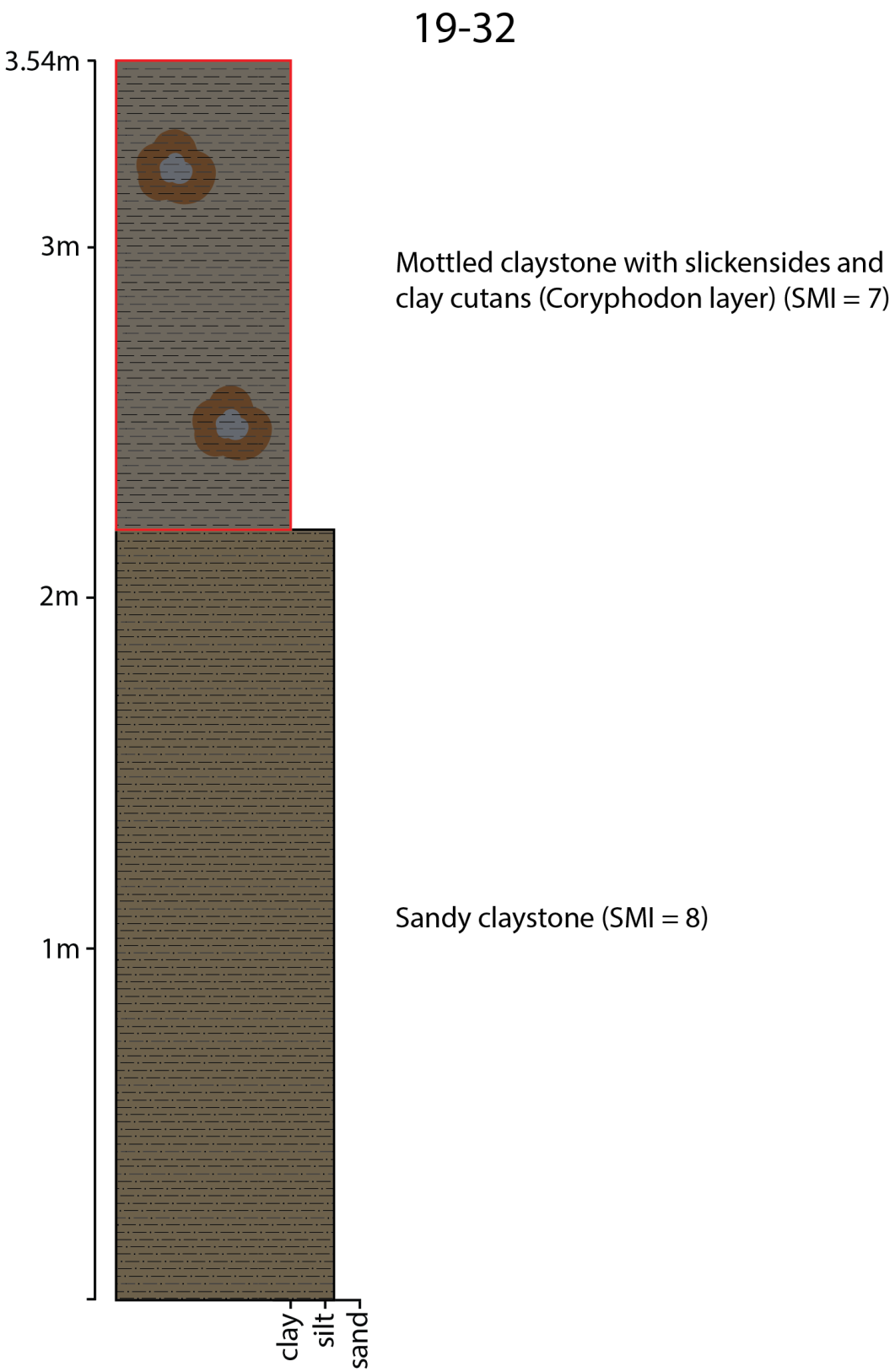

Figure 21. Column is CORY 19-32. See figure 12 for legend.

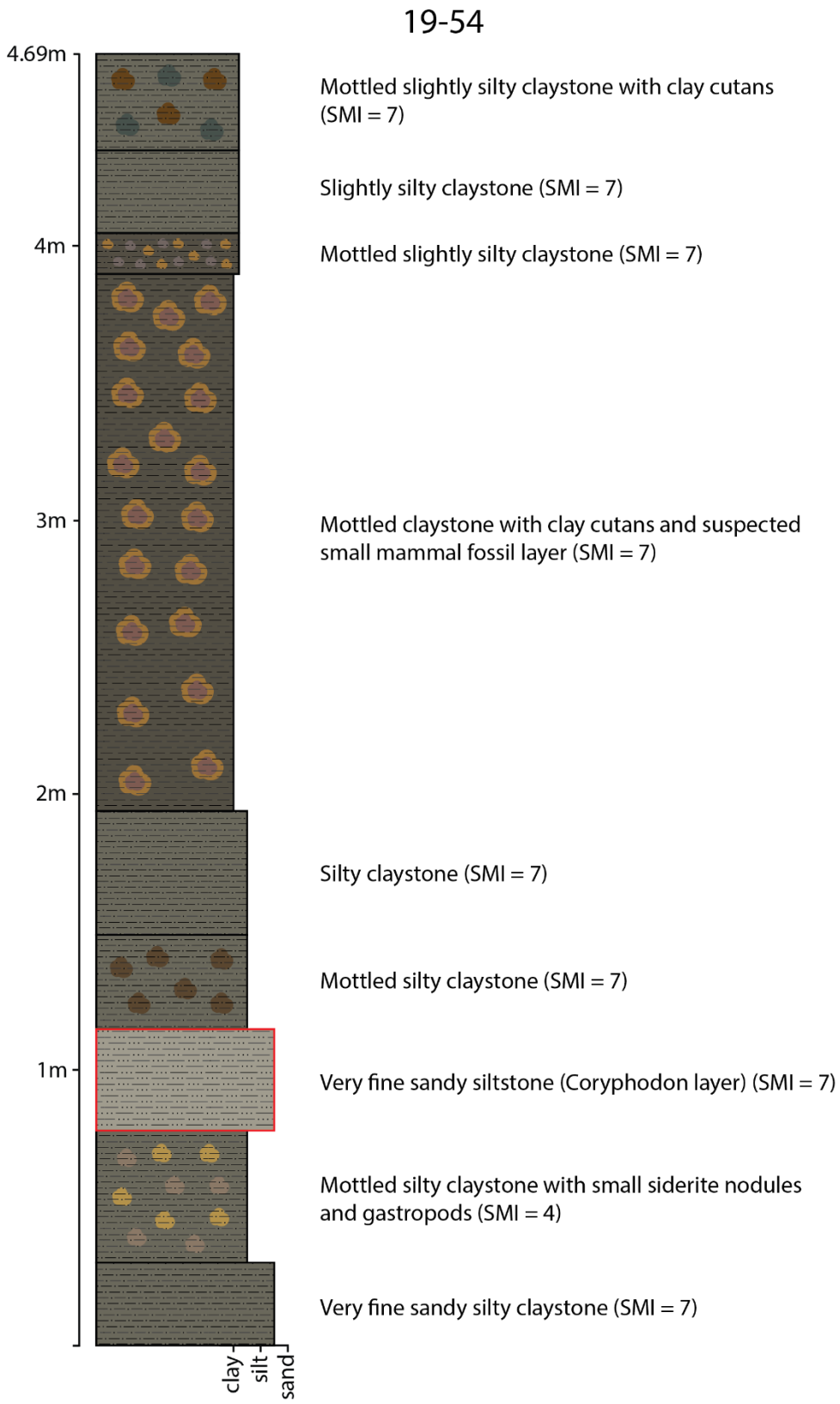

Figure 22. Column is CORY 19-54. See figure 12 for legend.

Wasatchian 1

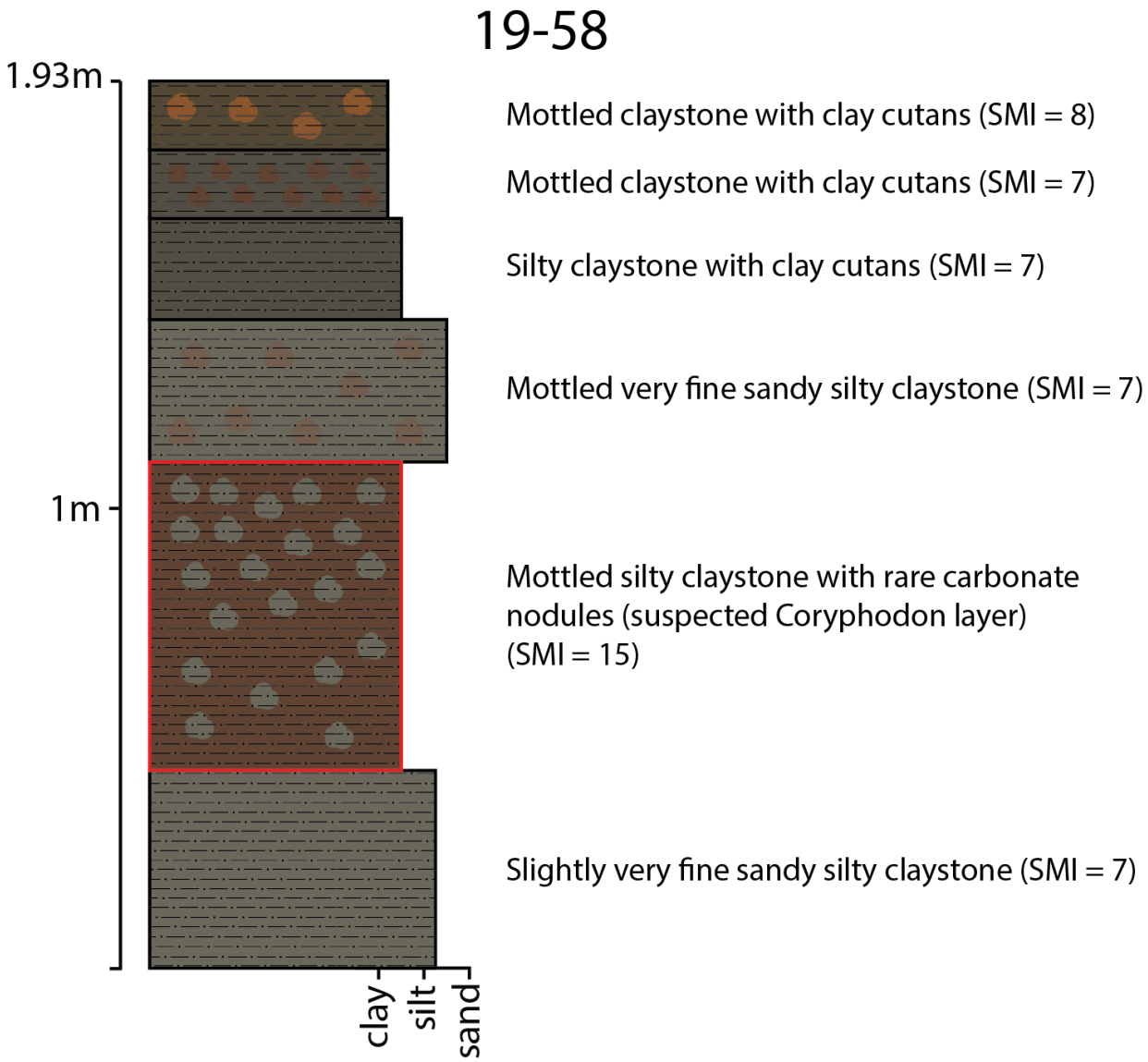

Figure 23. Column is CORY 19-58. See figure 12 for legend.

Wasatchian 2

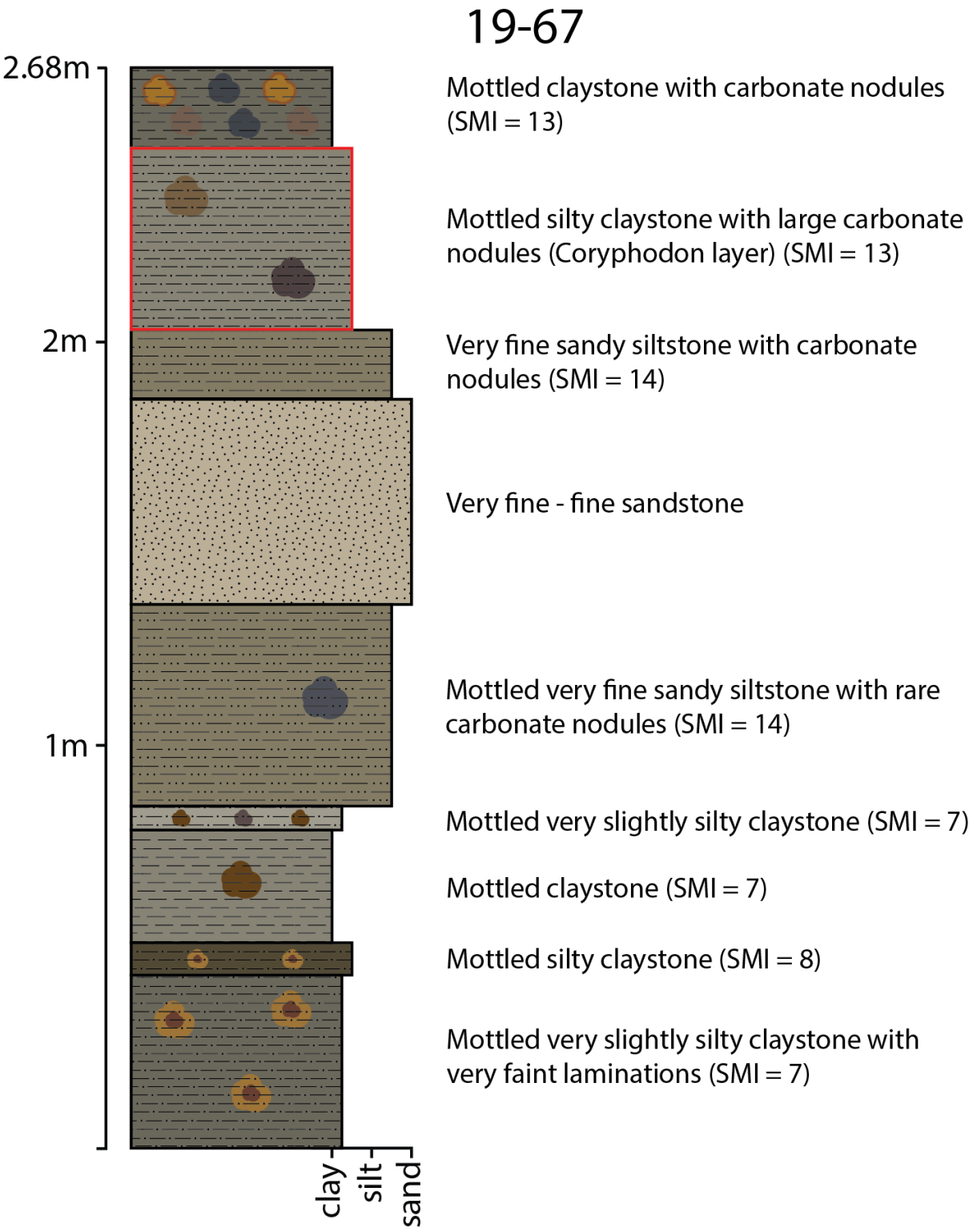

Figure 24. Column is CORY 19-67. See figure 12 for legend.

Wasatchian 4

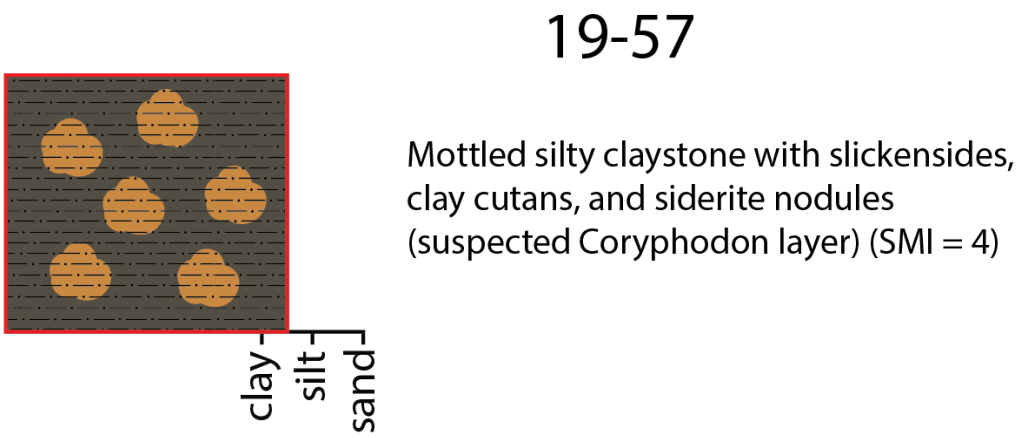

Figure 25. Column is CORY 19-57. The thickness of this unit is unknown. See figure 12 for legend.

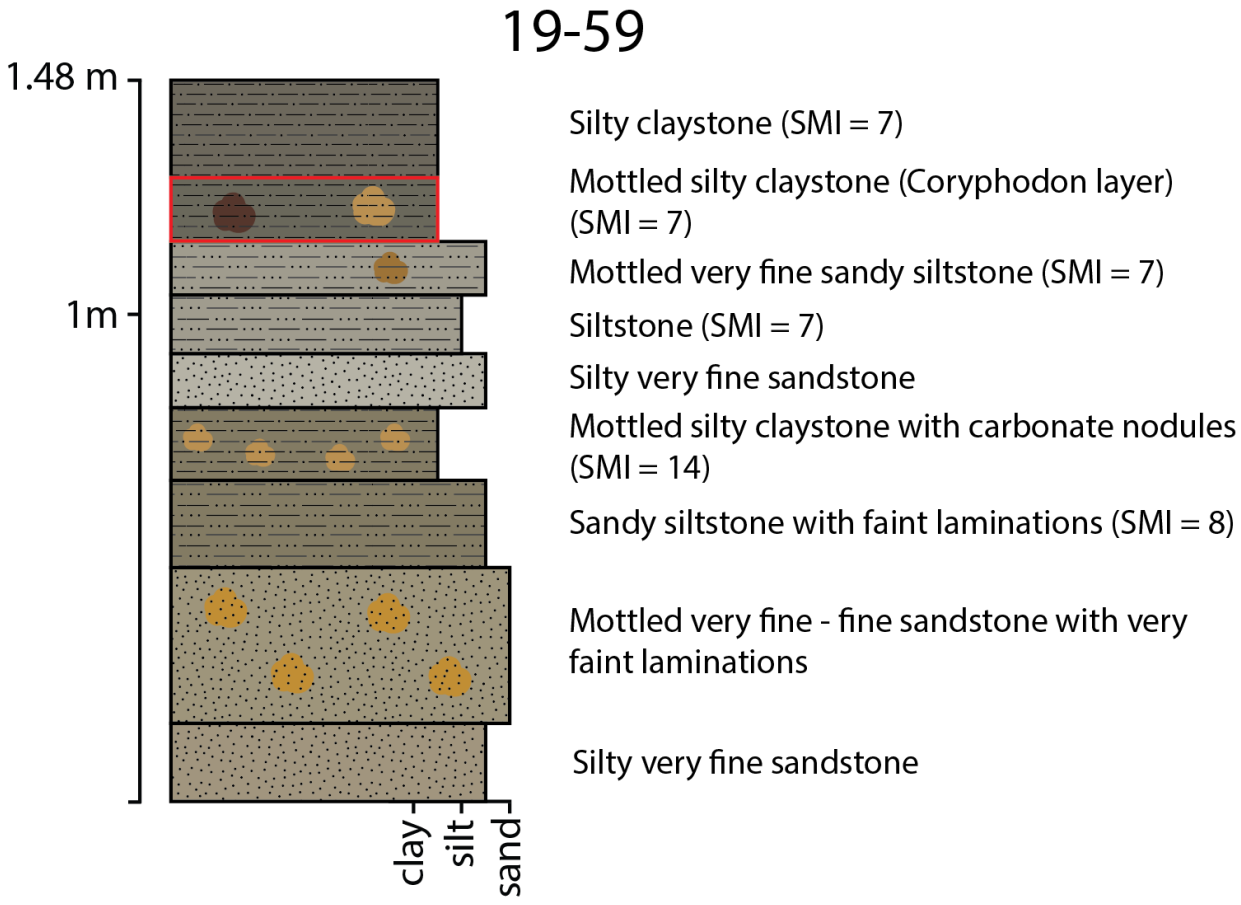

Figure 26. Column is CORY 19-59. See figure 12 for legend.

Soil Morphology Index (SMI) Numbers

SMI numbers were calculated for each *Coryphodon* unit. These were used to determine if there are statistically significant differences in the wetness of the paleoenvironments that *Coryphodon* fossils were deposited in between mammalian biozones (Figure 27). Higher numbers indicate dryer conditions while lower numbers indicate wetter ones. Lower numbers can be observed through the Clarkforkian, a large increase occurs in Wasatchian 1 and a large decrease in Wasatchian 4. Wasatchian 0 and 3 were not sampled.

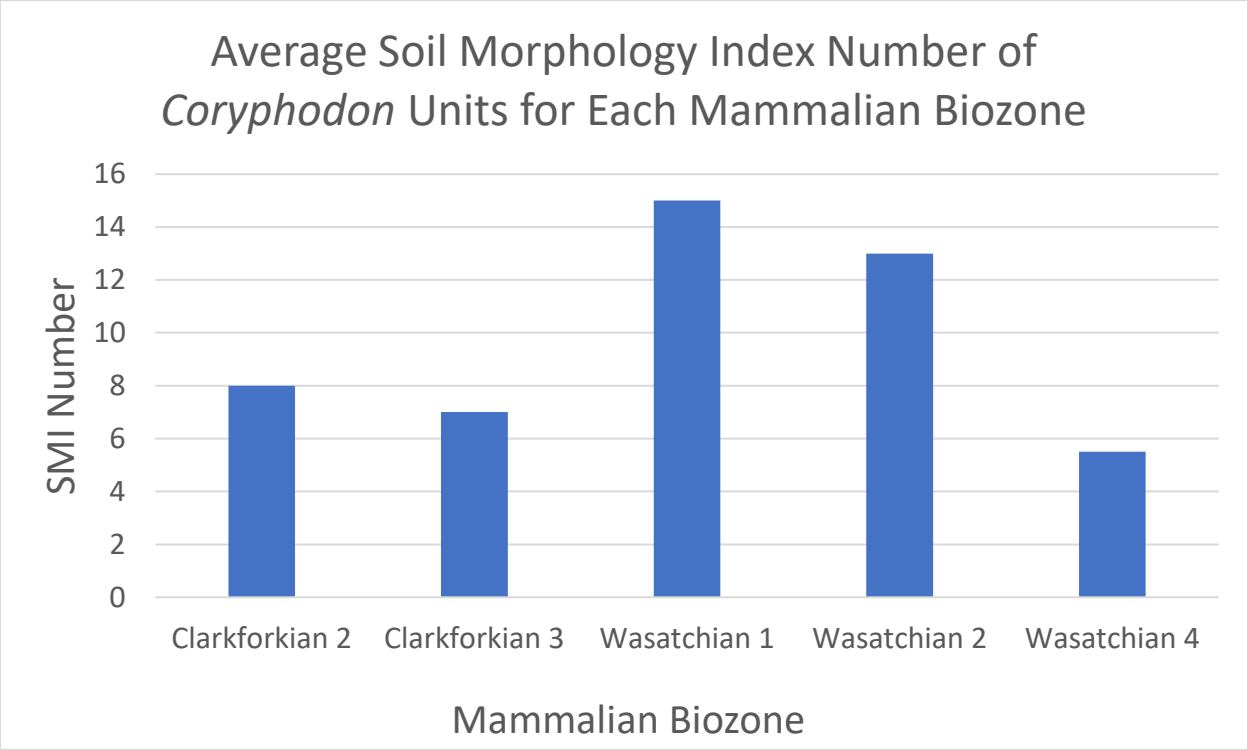

Figure 27. The average SMI number for the units containing *Coryphodon* in each mammalian biozone. A higher number represents a drier stratigraphic unit. The drying of the PETM interval can be observed between Clarkforkian 3 and Wasatchian 1, as there are no samples from Wasatchian 0. There are also no samples from Wasatchian 3.

Chi-Square Test

A chi-square test was run to determine if there is a relationship between the SMI numbers of *Coryphodon* units and the biozones these units are from (Figure 28). This test resulted in a significant result (p-value = 0.01379). Therefore, the null hypothesis can be rejected, which means that the distribution of counts across categories is not random, so SMI numbers of *Coryphodon* units are dependent on mammalian biozone. The residuals for a chi-square are the difference between the observed and expected counts by table cell. The greater that residual the more it affects the significance of the chi-square test. The residuals with the greatest contribution to the significant result are an SMI of 15 for Wasatchian 1 (residual contribution of 39.05%), an SMI of 13 for Wasatchian 2 (16.63%), an SMI of 4 for Wasatchian 4 (6.63%), an SMI of 5 for Clarkforkian 2 (5.78%), and an SMI of 7 for Clarkforkian 3 (3.85%).

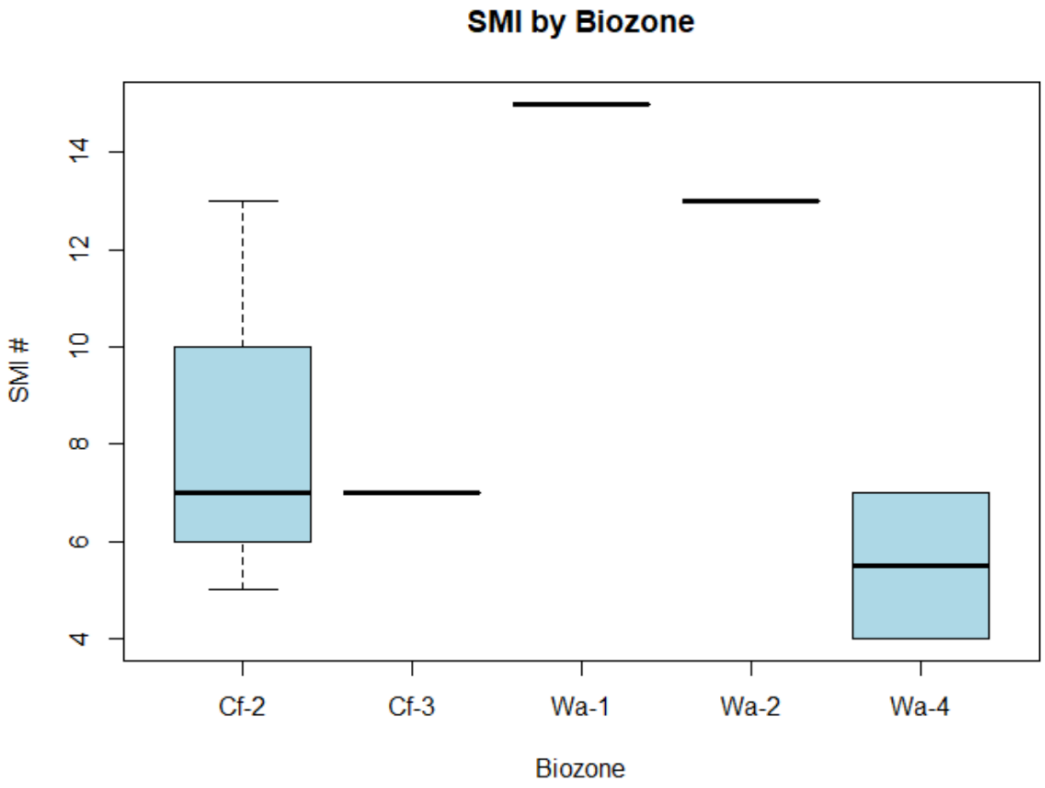

Figure 28. The spread of SMI numbers by biozone. Clarkforkian 3 has 6 *Coryphodon* bearing units but they all have the same SMI number. Wasatchian 1 and 2 only have one *Coryphodon* unit each.

ANOVA & Z-scores

The average SMI of the *Coryphodon* units in each biozone is normally distributed as shown by a Shapiro-Wilk test (W = 0.90198, p-value = 0.4209). Therefore, an ANOVA was run since that is parametric and assumes a normal distribution of the data. The ANOVA resulted in a significant result (p-value = 0.0196), which means that the null hypothesis can be rejected and the means of SMI values from at least one pairing of biozones from which these samples were drawn are significantly different. A Tukey test was then run to determine which pairing of biozones contained statistically different means of SMI values. The results showed that there is a significant difference between the SMI means of Clarkforkian 3 and Wasatchian 1 (p-value = 0.0414139) as well as Wasatchian 1 and Wasatchian 4 (p-value = 0.0325651). This is interesting as the PETM occurred between Clarkforkian 3 and Wasatchian 1, and Wasatchian 1 is before the PETM recovery interval whereas Wasatchian 4 is after that interval.

Z-score tests were also run between the SMIs of the biozones that the Tukey test found to be significantly different in order to verify these results. A Z-score above 1.96, which is the 95^{th} percentiles, means that the sample is statistically different from the population it is being compared to. In this case, the "population" is really just the samples in a different biozone that contains more than one sample. The SMI of the Wasatchian 1 sample is an outlier of the SMIs of the Wasatchian 4 "population", therefore they are statistically from different populations (Z-score = 4.478343). The same is true for the SMI of the Wasatchian 1 sample and the Clarkforkian 3 "population" (Z-score = 0, since the standard deviation is 0).

Mann-Whitney Test

A Mann-Whitney test was run to compare the SMI numbers of pre- and post-PETM stratigraphic units containing *Coryphodon*. This test was selected because the pre-PETM SMI numbers are not normally distributed (W = 0.54858, p-value = 1.357e-05). The test yielded a non-significant p-value of 0.5091. Therefore, the null hypothesis that the difference in the medians of these two variables is zero cannot be rejected. This means that the SMI numbers of the pre- and post-PETM stratigraphic units containing *Coryphodon* are not statistically significant from one another.

Discussion

My hypothesis, that the proposed semi-aquatic mammal *Coryphodon* would mainly be found in aquatic or semi-aquatic facies, is partly supported by the data. In the Clarkforkian 2 and 3 biozones, *Coryphodon* was found mainly in aquatic and semi-aquatic facies as well as in soils with evidence of wet and dry cycles, supporting my hypothesis. However, following the PETM, in Wasatchian 1, 2, and 4, there is only one instance of *Coryphodon* being found in a wetter soil, and no instances of it in a pond, swamp, or fluvial deposit (Table 2). This preliminary data suggest that *Coryphodon* was buried, and might have lived, in wetter habitats before the PETM, but was able to adapt to drier habitats post-PETM.

Biozone	Sampling Location	Paleoenvironmental Hypothesis
Wasatchian 4	19-59	Intermediate soil
Wasatchian 4	19-57	Wetter soil with wet and dry cycles
Wasatchian 2	19-67	Drier soil
Wasatchian 1	19-58	Drier soil
Clarkforkian 3	19-54	Fluvial deposit
Clarkforkian 3	19-32	Soil with wet and dry cycles
Clarkforkian 3	19-29	Pond or swamp
Clarkforkian 3	19-23	Soil with wet and dry cycles
Clarkforkian 3	19-22	Soil with wet and dry cycles
Clarkforkian 3	19-13	Soil with wet and dry cycles
Clarkforkian 2	19-52	Fluvial deposit
Clarkforkian 2	19-34	Drier soil
Clarkforkian 2	19-35	Swap or water-logged soil
Clarkforkian 2	19-53	Pond

Table 2. Paleoenvironmental interpretations based on soil features of the *Coryphodon* units in the measured stratigraphic columns, sorted from the youngest on top to oldest on bottom.

This potential shift in *Coryphodon* habitat preference, from aquatic and semi-aquatic to drier paleoenvironments, may be evidence that the changing paleoenvironment that *Coryphodon* lived in was in large part due to the PETM. However, it could also be that by increasing the sample size of units containing *Coryphodon*, specifically in the later biozone groupings that contain very few samples, they may be found in aquatic and semi-aquatic facies in these biozones as well. Additionally, it may be possible that they did live in these types of facies but were for some reason fossilized in or at least preserved better in soils as opposed to in swamps, ponds, and rivers in later biozones.

As the sample size of this study is relatively small, especially within biozone groupings, error is an important consideration. Wasatchian 0 and 3 were not represented and only one sample was collected for Wasatchian 1 and 2. Therefore, while preliminary data does show trends, even some that are significant, more data is crucial in order to increase the sample size and see if the observed differences of *Coryphodon* units between biozones still hold.

Additionally, the Soil Morphology Index (SMI) system, originally created by Adams et al. (2011), may not be the best way to numerically analyze the data from this area, as many of the layers do not contain any nodules, and the chroma only spanned 1 through 3. This meant that a large number of the *Coryphodon* bearing units have an SMI number between 6 and 8. Statistically, this means that the data is skewed towards these central SMI numbers despite the fact that there were paleoenvironmental changes between units with the same or very similar SMI numbers. This was particularly evident between soils that contained slickensides or clay cutans, and therefore indicated the presence of wet and dry cycles, and those that did not. It was also evident statistically when running a Mann-Whitney test to comparing the SMI numbers of the pre- and post-PETM stratigraphic units containing *Coryphodon*, as this test did not yield a significant result but when considering all observations there is a more obvious shift in the hypothesized paleoenvironments. Therefore, I propose that the presence or absence of additional sedimentary features, such as slickensides and clay cutans, may need to be included in calculating SMI numbers in order to have them better represent changing paleoenvironments as well as make it easier to statistically analyze the differences between these paleoenvironments.

Summary

1. My hypothesis was that the alleged semi-aquatic mammal *Coryphodon* would mainly be found in aquatic or semi-aquatic facies throughout the PETM interval.
2. Statistical analysis of soil morphology index (SMI) numbers indicate that there is a significant difference between the wetness of the paleoenvironments containing *Coryphodon* in mammalian biozones Clarkforkian 3 and Wasatchian 1, or before and after the main Paleocene-Eocene Thermal Maximum (PETM) interval, and Wasatchian 1 and Wasatchian 4, or pre- and post-PETM recovery interval. Based on our samples, *Coryphodon* is found in layers indicating a semi-aquatic habitat before the PETM but not afterward.
3. The number of samples in this study is small, especially after dividing samples into mammalian biozone groups. Therefore, more samples need to be collected and analyzed in order to increase confidence, both observationally and statistically, in the new hypothesis that *Coryphodon* lived in different paleoenvironments before and after the PETM.

References Cited

Abels, H.A., Lauretano, V., van Yperen, A.E., Hopman, T., Zachos, J.C., Lourens, L.J., Gingerich, P.D., and Bowen, G.J., 2016, Environmental impact and magnitude of paleosol carbonate carbon isotope excursions marking five early Eocene hyperthermals in the Bighorn Basin, Wyoming: Climate of the Past, v. 12, p. 1151–1163, doi:10.5194/cp-12-1151-2016.

Adams, J.S., Kraus, M.J., and Wing, S.L., 2011, Evaluating the use of weathering indices for determining mean annual precipitation in the ancient stratigraphic record: Palaeogeography, Palaeoclimatology, Palaeoecology, v. 309, p. 358–366, doi:10.1016/j.palaeo.2011.07.004.

Blakey, R.C., and Ranney, W.D., 2018, Flat-slab subduction, the Laramide Orogeny, uplift of the Colorado Plateau and Rocky Mountains: Paleocene and Eocene: ca. 65–35 Ma, *in* Blakey, R.C. and Ranney, W.D. eds., Ancient Landscapes of Western North America: A Geologic History with Paleogeographic Maps, New York, Springer International Publishing, p. 131–148, https://doi.org/10.1007/978-3-319-59636-5_9.

Blodgett, R.H., Crabaugh, J.P., and McBride, E.F., 1993, The color of red beds—a geologic perspective, *in* Bigham, J.M. and Ciolkosz, E.J. eds., Soil color, Madison, WI, Soil Science Society of America, v. 31, p. 127–159.

Bown, T.M., and Gingerich, P.D., 1980, The Willwood Formation (lower Eocene) of the southern Bighorn Basin, Wyoming, and its mammalian fauna, *in* Early Cenozoic paleontology and stratigraphy of the Bighorn Basin, Wyoming, University of Michigan Papers on Paleontology, v. 24, p. 127–146.

Butler, R.F., Lindsay, E.H., and Gingerich, P.D., 1981, Magnetic polarity stratigraphy and biostratigraphy of Paleocene and Lower Eocene continental deposits, Clark's Fork Basin, Wyoming: The Journal of Geology, v. 89, p. 299–316.

Carmichael, M.J. et al., 2017, Hydrological and associated biogeochemical consequences of rapid global warming during the Paleocene-Eocene Thermal Maximum: Global and Planetary Change, v. 157, p. 114–138.

Clementz, M.T., Holroyd, P.A., and Koch, P.L., 2008, Identifying aquatic habits of herbivorous mammals through stable isotope analysis: Palaios, v. 23, p. 574–585.

Clyde, W.C., Hamzi, W., Finarelli, J.A., Wing, S.L., Schankler, D., and Chew, A., 2007, Basin-wide magnetostratigraphic framework for the Bighorn Basin, Wyoming: GSA Bulletin, v. 119, p. 848–859, doi:10.1130/B26104.1.

Copeland, P., Currie, C.A., Lawton, T.F., and Murphy, M.A., 2017, Location, location, location: The variable lifespan of the Laramide orogeny: Geology, v. 45, p. 223–226, doi:10.1130/G38810.1.

D'Ambrosia, A.R., Clyde, W.C., Fricke, H.C., Gingerich, P.D., and Abels, H.A., 2017, Repetitive mammalian dwarfing during ancient greenhouse warming events: Science Advances, v. 3, p. 1–9.

DeCelles, P.G., 2004, Late Jurassic to Eocene evolution of the Cordilleran thrust belt and foreland basin system, western U.S.A.: American Journal of Science, v. 304, p. 105–168, doi:10.2475/ajs.304.2.105.

Dickinson, W., Klute, M., Hayes, M., Janecke, S., Lundin, E., McKittrick, M., and Olivares, M., 1988, Paleogeographic and paleotectonic setting of Laramide sedimentary basins in the central Rocky Mountain region: Geological Society of America Bulletin, v. 100, doi:10.1130/0016-7606(1988)100<1023:PAPSOL>2.3.CO;2.

Evans, C.V., and Franzmeier, D.P., 1986, Saturation, aeration, and color patterns in a toposequence of soils in north-central Indiana: Soil Science Society of America Journal, v. 50, p. 975–980, doi:10.2136/sssaj1986.03615995005000040029x.

Finn, T.M., 2010, Subsurface stratigraphic cross sections showing correlation of Cretaceous and lower Tertiary rocks in the Bighorn Basin, Wyoming and Montana: Geological Survey Digital Data Series DDS–69–V, p. 1–14.

Foreman, B.Z., 2014, Climate-driven generation of a fluvial sheet sand body at the Paleocene-Eocene boundary in north-west Wyoming (USA): Basin Research, v. 26, p. 225–241.

Gehler, A., Gingerich, P.D., and Pack, A., 2016, Temperature and atmospheric CO2 concentration estimates through the PETM using triple oxygen isotope analysis of mammalian bioapatite: Proceedings of the National Academy of Sciences, v. 113, p. 7739–7744, doi:10.1073/pnas.1518116113.

Gingerich, P.D., 1976, Cranial anatomy and evolution of early Tertiary Plesiadapidae (Mammalia, Primates): University of Michigan Papers on Paleontology, v. 15, p. 1–140.

Gingerich, P.D., 1980, Evolutionary patterns in early Cenozoic mammals: Annual Review of Earth and Planetary Sciences, v. 8, p. 407–424.

Gingerich, P.D., 2003, Mammalian responses to climate change at the Paleocene-Eocene boundary: Polecat Bench record in the northern Bighorn Basin, Wyoming, *in* Wing, S.L., Gingerich, P.D., Schmitz, B., and Thomas, E. eds., Causes and consequences of globally warm climates in the early Paleogene, Boulder, CO, Geological Society of America, Special Paper 369, p. 463–478.

Gingerich, P.D., 1989, New earliest Wasatchian mammalian fauna from the Eocene of northwestern Wyoming: composition and diversity in a rarely sampled high-floodplain assemblage: The University of Michigan, Papers on Paleontology, v. 28, p. 1–97.

Gingerich, P.D., 2019, Temporal scaling of carbon emission and accumulation rates: modern anthropogenic emissions compared to estimates of PETM-onset accumulation: Paleoceanography and Paleoclimatology, v. 34, p. 329–335, doi:10.1029/2018PA003379.

Gingerich, P.D., and Klitz, K., 1985, Paleocene and early Eocene fossil localities in the Fort Union and Willwood Formations, Clarks Fork Basin, Wyoming (map): University of Michigan Museum of Paleontology, https://deepblue.lib.umich.edu/handle/2027.42/48726 (accessed February 2020).

Kiehl, J.T., Shields, C.A., Snyder, M.A., Zachos, J.C., and Rothstein, M., 2018, Greenhouse- and orbital-forced climate extremes during the early Eocene: Philosophical Transactions of the Royal Society A: Mathematical, Physical and Engineering Sciences, v. 376, p. 1–24.

Kraus, M.J., McInerney, F.A., Wing, S.L., Secord, R., Baczynski, A.A., and Bloch, J.I., 2013, Paleohydrologic response to continental warming during the Paleocene-Eocene Thermal Maximum, Bighorn Basin, Wyoming: Palaeogeography, Palaeoclimatology, Palaeoecology, v. 370, p. 196–208.

Kraus, M.J., and Riggins, S., 2007, Transient drying during the Paleocene–Eocene Thermal Maximum (PETM): Analysis of paleosols in the Bighorn Basin, Wyoming: Palaeogeography, Palaeoclimatology, Palaeoecology, v. 245, p. 444–461.

Kraus, M.J., and Wells, T.M., 1999, Facies and facies architecture of Paleocene floodplain deposits, Fort Union Formation, Bighorn Basin, Wyoming: The Mountain Geologist, v. 36, p. 57–70.

Kraus, M.J., Woody, D.T., Smith, J.J., and Dukic, V., 2015, Alluvial response to the Paleocene–Eocene Thermal Maximum climatic event, Polecat Bench, Wyoming (U.S.A.): Palaeogeography, Palaeoclimatology, Palaeoecology, v. 435, p. 177–192.

Mackin, J.H., 1937, Erosional history of the Big Horn Basin, Wyoming: GSA Bulletin, v. 48, p. 813–894, doi:10.1130/GSAB-48-813.

McInerney, F.A., and Wing, S.L., 2011, The Paleocene-Eocene Thermal Maximum: A perturbation of carbon cycle, climate, and biosphere with implications for the future: Annual Review of Earth and Planetary Sciences, v. 39, p. 489–516, doi:10.1146/annurev-earth-040610-133431.

PiPujol, M.D., and Buurman, P., 1994, The distinction between ground-water gley and surface-water gley phenomena in Tertiary paleosols of the Ebro basin, NE Spain: Palaeogeography, Palaeoclimatology, Palaeoecology, v. 110, p. 103–113, doi:10.1016/0031-0182(94)90112-0.

Retallack, G.J., 1994, The environmental factor approach to the interpretation of paleosols, *in* Amundson, R.R., Harden, J., and Singer, M. eds., Factors of soil formation: a fiftieth anniversary retrospective, Madison, WI, Soil Science Society of America, v. 33, p. 31–64.

Retallack, G.J., 1991, Untangling the effects of burial alteration and ancient soil formation: Annual Review of Earth and Planetary Sciences, v. 19, p. 183–206, doi:10.1146/annurev.ea.19.050191.001151.

Rose, K.D., 1980, Clarkforkian land-mammal age: Revised definition, zonation, and tentative intercontinental correlations: Science, v. 208, p. 744–746, doi:10.1126/science.208.4445.744.

Royer, D.L., 1999, Depth to pedogenic carbonate horizon as a paleoprecipitation indicator? Geology, v. 27, p. 1123–1126, doi:10.1130/0091-7613(1999)027<1123:DTPCHA>2.3.CO;2.

Schmidt, D.N., Thomas, E., Authier, E., Saunders, D., and Ridgwell, A., 2018, Strategies in times of crisis—insights into the benthic foraminiferal record of the Palaeocene–Eocene Thermal Maximum: Philosophical Transactions of the Royal Society A: Mathematical, Physical and Engineering Sciences, v. 376, p. 1–17.

Schwertmann, U., and Fanning, D.S., 1976, Iron-manganese concretions in hydrosequences of soils in loess in Bavaria: Soil Science Society of America Journal, v. 40, p. 731–738, doi:10.2136/sssaj1976.03615995004000050034x.

Secord, R., Bloch, J.I., Chester, S.G.B., Boyer, D.M., Wood, A.R., Wing, S.L., Kraus, M.J., McInerney, F.A., and Krigbaum, J., 2012, Evolution of the earliest horses driven by climate change in the Paleocene-Eocene Thermal Maximum: Science, v. 335, p. 959–962.

Secord, R., Gingerich, P., Smith, M., Clyde, W., Wilf, P., and Singer, B., 2006, Geochronology and mammalian biostratigraphy of Middle and Upper Paleocene continental strata, Bighorn Basin, Wyoming: Papers in the Earth and Atmospheric Sciences, https://digitalcommons.unl.edu/geosciencefacpub/190.

Seeland, D., 1998, Late Cretaceous, Paleocene, and early Eocene paleogeography of the Bighorn Basin and northwestern Wyoming: v. 49, p. 137–165.

Simons, E.L., 1960, The Paleocene Pantodonta: Transactions of the American Philosophical Society, v. 50, p. 3–99.

Smith, J.J., Hasiotis, S.T., Kraus, M.J., and Woody, D.T., 2009, Transient dwarfism of soil fauna during the Paleocene–Eocene Thermal Maximum: Proceedings of the National Academy of Sciences, v. 106, p. 17655–17660.

Smith, J.J., Hasiotis, S.T., Woody, D.T., and Kraus, M.J., 2008, Paleoclimatic implications of crayfish-mediated prismatic structures in paleosols of the Paleogene Willwood Formation, Bighorn Basin, Wyoming, U.S.A.: Journal of Sedimentary Research, v. 78, p. 323–334.

Tauxe, L., Gee, J., Gallet, Y., Pick, T., and Bown, T., 1994, Magnetostratigraphy of the Willwood Formation, Bighorn Basin, Wyoming: new constraints on the location of Paleocene/Eocene boundary: Earth and Planetary Science Letters, v. 125, p. 159–172.

Uhen, M.D., and Gingerich, P.D., 1995, Evolution of *Coryphodon* (Mammalia, Pantodonta) in the late Paleocene and early Eocene of northwestern Wyoming: Contributions from the Museum of Paleontology, University of Michigan, v. 29, p. 259–289.

Veneman, P.L.M., Spokas, L.A., and Lindbo, D.L., 1998, Soil moisture and redoximorphic features: a historical perspective, *in* Rabenhorst, M.C., Bell, J.C., and McDaniel, P.A. eds., Quantifying soil hydromorphology, Madison, WI, Soil Science Society of America, v. 54, p. 1–23.

Wing, S.L., Harrington, G.J., Smith, F.A., Bloch, J.I., Boyer, D.M., and Freeman, K.H., 2005, Transient floral change and rapid global warming at the Paleocene-Eocene boundary: Science, v. 310, p. 993–996.

Appendix

Specimen #	Locality #	Formation	Fossil ID	Unit #	Thickness (m)	Grain Size
CORY 19-13	SH-07	Willwood (Paleocene)	*Coryphodon* parts of femur and phalanges	2	0.05	VF sandy siltstone
				3	0.7	Slightly silty claystone
				4	0.28	Silty claystone
				5	0.29	Siltstone
				6	0.19	Silty claystone
				7	0.61	Siltstone
				8	0.2	Claystone
				9	0.41	Siltstone
CORY 19-22	RG-03	Willwood (Paleocene)	Complete *Coryphodon* tibia	1	1.17	Massive clay siltstone
				2	0.7	Mudstone
				3	0.41	Silty claystone
CORY 19-23	MD-04	Willwood (Paleocene)	*Coryphodon* ? - canine, phalanx, and other bones	1	Claystone	
CORY 19-29	SH-01	Willwood (Paleocene)	*Coryphodon* skull with ulna	4	~0.4-0.5	Silty claystone
CORY 19-32	KS-01	Willwood (Paleocene)	*Coryphodon* canine - other specimens include possible pelvis, vertebrae, teeth, hand or foot, other small mammals, croc, turtle	1	2.2	Massive sandy claystone
				2	1.34	Claystone
CORY 19-34	MF-08	Willwood (Paleocene)	*Coryphodon* post crania	*Coryphodon* Layer	Silty claystone	
CORY 19-35	MD-02	Willwood (Paleocene)	*Coryphodon* teeth & skull fragments	1	0.1	VF sandy siltstone
				2	0.16	Siltstone
				3	0.25	Silty claystone
				4	0.09	Claystone
				5	At least 0.25	Claystone
CORY 19-52	MD-09	Willwood (Paleocene)	*Coryphodon* teeth	1	0.25	Silty claystone
				2	0.42	Massive sandy siltstone
				3	0.19	Claystone
				4	0.35	Claystone
				5	0.25	Slightly silty claystone
				6	1.8	VF sandy siltstone
				7	1.32	Massive silty VF sandstone
				8	At least 0.2	Claystone
CORY 19-53	TC-01	Willwood (Paleocene)	*Coryphodon* teeth	1	At least 0.34 m, base not exposed	Massive VF sandstone
				2	0.62 m (from one trench to another)	Silty claystone
				3	0.13	Claystone
				4	0.07	Massive sandy mudstone
				5	0.18	Silty claystone
				6	0.13	Massive slightly silty claystone
				7	0.11	Mudstone
				8	0.14	Massive clay siltstone
				9	0.14	Silty claystone
				10	0.32	Sandy claystone
				11	0.03	Massive slightly silty claystone
CORY 19-54	ER-04	Willwood (Eocene)	*Coryphodon* post crania, humeral head, proximal tibia, tarsal, distal ulna & other small mammal bones	12	0.47	Massive silty claystone
				1	0.3	Massive VF sandy silty claystone
				2	0.48	Silty claystone
				3	0.37	Massive VF sandy siltstone
				4	0.34	Silty claystone
				5	0.45	Massive silty claystone
				6	1.95	Claystone
				7	0.15	Slightly silty claystone
				8	0.3	Slightly silty claystone
				9	0.35	Slightly silty claystone
CORY 19-57	MF-05	Willwood (Eocene)	*Coryphodon* skeleton	*Coryphodon* Layer	Silty claystone	
CORY 19-58	MF-07	Willwood (Eocene)	Exploded *Coryphodon* skeleton: vertebrae, phalanges, ribs, femeral head, distal end of tibia and possible radius	1	0.43	Massive slightly VF sandy silty claystone
				2	0.67	Silty claystone
				3	0.31	VF sandy silty claystone
				4	0.22	Silty claystone
				5	0.15	Claystone
CORY 19-59	IS-07	Willwood (Eocene)	*Coryphodon* teeth	6	At least 0.15	Claystone
				1	0.16	Silty VF sandstone
				2	0.32	VF-F sandstone
				3	0.18	Massive sandy siltstone
				4	0.15	Silty claystone
				5	0.11	Silty VF sandstone
				6	0.12	Massive siltstone
				7	0.11	VF sandy siltstone
				8	0.13	Silty claystone
				9	At least 0.2	Massive silty claystone
CORY 19-67	MD-19	Willwood	*Coryphodon* - femur, humerus, and tooth fragments	1	0.43	Very slightly silty claystone
				2	0.08	Silty claystone
				3	0.28	Claystone
				4	0.06	Very slightly silty claystone
				5	0.5	VF sandy siltstone
				6	0.51	VF-F sandstone
				7	0.17	VF sandy siltstone
				8	0.45	Silty claystone
				9	At least 0.2	Claystone

Matrix Color 1	Matrix Color 2	Matrix Color Notes	Chroma (SMI)	Mottling (%)	Mottling Color 1	Mottling Color 2	Mottling Color 3	Mottling Color 4	Mottling Color Notes
Olive gray 5Y 5/2			2	15	Strong brown 7.5YR 4/6				
Olive gray 5Y 4/2			2	30	Dark reddish gray 10R 3/1	Yellowish brown 10YR 5/6			
Light olive gray 5Y 6/2			2	5	Yellowish brown 10YR 5/8	Pale red 5R 7/2			Color 1 stronger, color 2 very faint
Dark gray 5Y 4/1			1	weak	Yellowish brown 10YR 5/4	Dark reddish gray 10R 3/1			
Very dark gray 5Y 3/1			1	15	Strong brown 7.5YR 5/8				
Light olive gray 5Y 6/2			2	30	Yellowish brown 10YR 5/8				
Dark gray 5Y 4/1			1	rare	Dark reddish gray 10R 3/1	Dark yellowish brown 10YR 4/6			
Light olive gray 5Y 6/2			2	3	Pale olive 5Y 6/4				
Very dark gray 7.5YR 3/1			1	7	Dark brown 7.5YR 3/3	Dark reddish gray 10R 3/1			
Dark gray 5Y 4/1			1	35	Strong brown 7.5YR 4/6	Dark reddish brown 5YR 3/3	Very dark bluish gray GLEY 2 (5PB) 3/1		
Dark gray 10YR 4/1			1	20	Dark bluish gray GLEY 2 (5PB) 4/1				
Dark gray 2.5Y 4/1			1	10	Brown 7.5YR 4/4				
Dark gray 5Y 4/1			1	0	N/A				
Dark grayish brown 2.5Y 4/2			2	0	N/A				
Dark gray 10YR 4/1			1	5	Dark brown 7.5YR 3/4	Dark bluish gray GLEY 2 (5PB) 4/1			
Very dark gray 5Y 3/1			1	10	Pale olive 5Y 6/4	Very dark bluish gray GLEY 2 (5PB) 3/1			
Light olive gray 5Y 6/2			2	15	Dark yellowish brown 10YR 4/6				
Dark olive gray 5Y 3/2			2	10	Strong brown 7.5YR 4/6				
Black 5Y 2.5/2			2	5	Dark yellowish brown 10YR 4/6				
Light olive gray 5Y 6/2	Dark gray 5Y 4/1	Faintly mottled w/ color 2	2	5	Strong brown 7.5YR 4/6				
Dark gray 5Y 4/1	Light olive gray 5Y 6/2	A bit of mottled color 2	1	15	Yellowish brown 10YR 5/6				
Olive gray 5Y 5/2			2	50	Dark reddish brown 5YR 3/3	Light yellowish brown 2.5Y 6/4			
Gray 5Y 5/1			1	0	N/A				
Dark reddish brown 2.5YR 3/3			3	30	Brown 7.5YR 4/4	Gray 5Y 5/1			
Gray 5Y 5/1			1	15	Reddish brown 5YR 4/4				
Very dark gray 5Y 3/1			1	10	Dark reddish brown 2.5YR 3/4				
Dark gray 5Y 4/1			1	10	Dark reddish gray 5R 3/1	Strong brown 7.5YR 5/8			
Gray 2.5Y 6/1			N/A	0	N/A				
Dark gray 5Y 4/1			1	10	Dark reddish brown 5YR 3/4	Dark yellowish brown 10YR 4/4	Dark reddish gray 10R 3/1		
Gray 5Y 5/1			N/A	0	N/A				
Dark gray 2.5Y 4/1			1	5	Dark reddish brown 2.5YR 3/3				
Very dark gray 2.5Y 3/1			1	0	N/A				
Very dark gray 5Y 3/1			1	0	N/A				
Gray 10YR 5/1			1	5	Yellowish brown 10YR 5/4				
Very dark gray 5Y 3/1			1	0	N/A				
Very dark gray 10YR 3/1			1	1	Yellowish brown 10YR 5/6				
Gray 10YR 5/1			1	0	N/A				
Very dark gray 10YR 3/1			1	3	Yellowish brown 10YR 5/6				
Light brownish gray 2.5Y 6/2			2	0	N/A				
Dark grayish brown 2.5Y 4/2			2	0	N/A				
Dark grayish brown 2.5Y 4/2			2	0	N/A				
Dark gray 5Y 4/1			1	0	N/A				
Dark gray 5Y 4/1			1	25	Grayish brown 10YR 5/2	Olive yellow 2.5Y 6/6			Very little of color 2
Gray 5Y 6/1			1	0	N/A				
Dark gray 5Y 4/1			1	15	Dark brown 10YR 3/3				
Dark gray 5Y 4/1			1	0	N/A				
Very dark gray 5Y 3/1			1	50 (top) –> 30 (bottom)	Yellowish brown 10YR 5/6	Weak red 10R 4/3			
Very dark gray 2.5Y 3/1			1	35	Yellowish brown 10YR 5/6	Dark reddish gray 10R 4/1			
Dark gray 5Y 4/1			1	0	N/A				
Dark gray 5Y 4/1			1	15	Dark yellowish brown 10YR 3/6	Very dark gray GLEY 1 (5G) 3/1			
Very dark gray 2.5Y 3/1			1	15	Reddish yellow 7.5YR 6/8				
Dark gray 5Y 4/1			1	0	N/A				
Dark reddish brown 5YR 3/3			3	50 (top) –> 20 (bottom)	Dark gray 5Y 4/1				
Dark gray 5Y 4/1			1	20	Brown 7.5YR 4/2				
Very dark gray 5Y 3/1			1	0	N/A				
Very dark gray 2.5Y 3/1			1	25	Dark reddish brown 5YR 3/3				
Very dark grayish brown 2.5Y 3/2			2	10	Yellowish red 5YR 4/6				
Light brownish gray 2.5Y 6/2			N/A	0	N/A				
Light olive gray 5Y 6/2			N/A	10	Brownish yellow 10YR 6/8				
Olive gray 5Y 5/2			2	0	N/A				
Olive gray 5Y 5/2			2	10	Brownish yellow 10YR 6/6				
Light gray 5Y 7/1			N/A	0	N/A				
Gray 5Y 6/1			1	0	N/A				
Gray 5Y 6/1			1	2	Yellowish brown 10YR 5/6				
Dark gray 5Y 4/1			1	5	Dark reddish brown 2.5YR 2.5/3	Brownish yellow 10YR 6/6			
Dark gray 2.5Y 4/1			1	0	N/A				
Dark gray 5Y 4/1			1	7	Yellowish brown 10YR 5/6	Dark reddish brown 2.5YR 3/4			
Dark olive gray 5Y 3/2			2	4	Yellowish brown 10YR 5/6	Dark reddish brown 2.5YR 3/4			
Gray 5Y 5/1			1	3	Dark yellowish brown 10YR 3/6				
Gray 5Y 6/1	Dark gray 5Y 4/1	Mottled	1	7	Dark yellowish brown 10YR 3/6	Dark reddish gray 7.5R 3/1			
Olive gray 5Y 5/2			2	1	Very dark bluish gray GLEY 2 (5PB) 3/1				
Light gray 2.5Y 7/2			N/A	0	N/A				
Olive gray 5Y 5/2			2	0	N/A				
Gray 5Y 5/1			1	5	Brown 10YR 4/3	Reddish black 5R 2.5/1			
Dark gray 5Y 4/1			1	15	Yellowish red 5YR 4/6	Yellowish brown 10YR 5/8	Bluish black GLEY 2 (5PB) 2.5/1	Brown 7.5YR 4/2	

Slickensides	Clay Cutans	Nodules	Nodule Fizz & Notes	Nodule ID	Carbonate Nodules (SMI)	Siderite Nodules (SMI)	Lower Contact	Soil Morphology Index #	Notes on Possible Depositional Environment
N	N	N			0	6	Abrupt	8	
N	N	N			0	6	Abrupt	8	Soil horizon
N	N	N			0	6	Gradational	8	Weak soil horizon
N	N	N			0	6	Gradational	7	
N	Y	N			0	6	Gradational	7	
N	N	N			0	6	Gradational	8	
N	N	N			0	6	Gradational	7	
Y	N	N			0	6	Gradational	8	
Y	N	N			0	6	Gradational	7	Weak, poorly drained soil, probably a C-horizon
Y	N	N			0	6	Gradational	7	Better drained/longer timed interval soil horizon, probably B-horizon
Y (small)	Y	N			0	6	Gradational	7	Poorly drained soil (less than 2), B-horizon
Y	N	N			0	6	N/A	7	Poorly drained soil
Y	N	N			0	6		7	Poorly drained floodplain, likely pond margin
N	N	N			0	6	N/A	8	Crevasse splay
Y	Y	N			0	6		7	Poorly drained soil
N	N	Y	Heavy fizz	Carbonate	6	6	N/A	13	
N	N	N			0	6	N/A	8	
N	N	Y	Very little fizz	Siderite	0	3	Gradational	5	
N	N	N			0	6	Gradational	8	
N	N	N			0	6	Abrupt	8	
N	Y	Y (small)	Very little fizz	Siderite	0	3	Abrupt	4	
Y (small)	N	N			0	6	N/A	8	Soil horizon
N	N	N			0	6	Abrupt	7	
N	Y	N			0	6	Abrupt	9	
Y	Y (lots)	N			0	6	Gradational	7	Soil horizon
N	N	N			0	6	Abrupt	7	
Y (weak)	N	N			0	6	Abrupt	7	
N	N	Possible			N/A	N/A	Abrupt	N/A	Fluvial channel
Y (weak)	Y	N			0	6	Abrupt	7	
N	N	N			N/A	N/A	N/A	N/A	
Y	Y	N			0	6	Gradational	7	Possibly a pedogenically modified pond
N	N	N			0	6	Gradational	7	
N	N	N			0	6	Gradational	7	
N	Y	N			0	6	Gradational	7	
N	Y	N			0	6	Gradational	7	
Y	Y (large)	N			0	6	Gradational	7	
N	N	N			0	6	Abrupt	7	
N	Y	N			0	6	Gradational	7	
N	Y	N			0	6	Gradational	8	
N	N	N			0	6	Abrupt	8	
N	Y	Y	Heavy fizz, not so much in some places	Carbonate	6	6	Abrupt	14	
N	N	N			0	6	N/A	7	
N	N	Y (small)	Low levels of fizzing	Siderite	0	3	Gradational	4	
N	N	N			0	6	Abrupt	7	
N	N	N			0	6	Abrupt	7	
N	N	N			0	6	Abrupt	7	
N	Y	N			0	6	Gradational	7	
N	N	N			0	6	Very abrupt	7	
N	N	N			0	6	Gradational	7	
N	Y	N			0	6	Gradational	7	
Y	Y	Y	Relatively low fizzing, more orange	Siderite	0	3	N/A	4	
N	N	N			0	6	N/A	7	
N	N	Rare (medium)	Heavy fizz	Carbonate	6	6	Abrupt	15	
N	N	N			0	6	Gradational	7	
N	Y	N			0	6	Gradational	7	
N	Y	N			0	6	Abrupt	7	Soil horizon
N	Y	N			0	6	Gradational	8	Soil horizon
N	N	Possible			N/A	N/A	N/A	N/A	
N	N	N			N/A	N/A	Abrupt	N/A	
N	N	N			0	6	Gradational	8	
N	N	Y	Heavy fizz	Carbonate	6	6	Abrupt	14	
N	N	N			N/A	N/A	Gradational	N/A	
N	N	N			0	6	Gradational	7	
N	N	N			0	6	Abrupt	7	
N	N	N			0	6	Abrupt	7	
N	N	N			0	6	Gradational	7	
N	N	N			0	6	N/A	7	
N	N	N			0	6	Gradational	8	
N	N	N			0	6	Gradational	7	
N	N	N			0	6	Abrupt	7	
N	N	Y (rare)	Heavy fizz	Carbonate	6	6	Gradational	14	
N	N	N			N/A	N/A	Abrupt	N/A	
N	N	Y (abundant & vary in size)	Heavy fizz	Carbonate	6	6	Abrupt	14	
N	N	Y (larger but less abundant)	Heavy fizz	Carbonate	6	6	Gradational	13	
N	Y	Y (abundant & vary in size)	Heavy fizz	Carbonate	6	6	Abrupt	13	Soil horizon

Other Notes & Fossil Layers	Histology
	Femur
Crushed bivalves in lower part of unit	
Suspected *Coryphodon* fossil layer	
	Tibia
Gastropods, *Coryphodon* fossils from this unit	
Had organic material, *Coryphodon* fossils from this unit	Canine
10-15% sand, relatively homogenous, but slight coarsening upwards	Canine
Coryphodon fossils from the base of this unit	
Same strat column as MD-09, *Coryphodon* fossil layer	
	Canine
Coryphodon fossil layer, huge gastropod, some charcoal	
Lots of smaller gastropods	
	Possible
Coryphodon fossil layer	
Croc fossil layer	
Horse fossil layer	
No bedding or sed structures	Premolar and incisor
Coryphodon fossils and shells were found in this layer	
Shells/gastropods present	
Gastropods	
Bioturbation present, slightly coarser near the top	
Gastropods (lots of them)	
	Possible
Some gastropods	
Coryphodon fossil layer	
Likely small mammal fossil layer because of their red color, Mottling decreases and gets less orange and more red going down (gradational change)	
Probably *Coryphodon* fossil layer, similarity in color to bones and highers layer with articulated bone exposed on surface	Possible
	Planned - radius and possible tibia
Similar in color to *Coryphodon* fossils, so likely from the layer	
Very faint laminations, mottling more common in some areas than others	
Faint laminations	
Coryphodon fossil layer	
Very faint laminations	
Coryphodon fossil layer	